© 2019. Published by The Company of Biologists Ltd | Development (2019) 146, dev172668. doi:10.1242/dev.172668

STEM CELLS AND REGENERATION

RESEARCH ARTICLE

Laminin α2 controls mouse and human stem cell behaviour during midbrain dopaminergic neuron development

Maqsood Ahmed[1,*], Leandro N. Marziali[2], Ernest Arenas[3], M. Laura Feltri[2] and Charles ffrench-Constant[1]

ABSTRACT

Development of the central nervous system requires coordination of the proliferation and differentiation of neural stem cells. Here, we show that laminin alpha 2 (lm-α2) is a component of the midbrain dopaminergic neuron (mDA) progenitor niche in the ventral midbrain (VM) and identify a concentration-dependent role for laminin α2β1γ1 (lm211) in regulating mDA progenitor proliferation and survival via a distinct set of receptors. At high concentrations, lm211-rich environments maintain mDA progenitors in a proliferative state via integrins α6β1 and α7β1, whereas low concentrations of lm211 support mDA lineage survival via dystroglycan receptors. We confirmed our findings *in vivo*, demonstrating that the VM was smaller in the absence of lm-α2, with increased apoptosis; furthermore, the progenitor pool was depleted through premature differentiation, resulting in fewer mDA neurons. Examination of mDA neuron subtype composition showed a reduction in later-born mDA neurons of the ventral tegmental area, which control a range of cognitive behaviours. Our results identify a novel role for laminin in neural development and provide a possible mechanism for autism-like behaviours and the brainstem hypoplasia seen in some individuals with mutations of *LAMA2*.

KEY WORDS: Extracellular matrix, Neural stem cells, Laminin, Integrin, Dystroglycan, Dopaminergic neurons, Congenital muscular dystrophy

INTRODUCTION

During development, the embryonic central nervous system (CNS) consists of proliferating neural stem cells (NSCs) that are exposed to a balance of intrinsic and extrinsic factors that regulate cell fate decisions (Ahmed and ffrench-Constant, 2016; Rozario and DeSimone, 2010). One such extrinsic determinant is the extracellular matrix (ECM), a multifunctional network of proteins interacting with and regulating a range of cell functions. Transcriptional analysis of mouse and human neocortices display an enrichment of ECM genes such as those encoding laminins, proteoglycans and integrins in the germinal zones, which suggests they play a role in regulating NSC behaviour (Fietz et al., 2012; Pollen et al., 2015).

Laminins are high molecular weight, heterotrimeric glycoproteins composed of α, β and γ chains. To date, five α, three β and three γ chains have been identified, combining to form at least 16 different combinations in the mouse, creating considerable tissue heterogeneity. Mutations to the human gene (*LAMA2*) encoding laminin alpha 2 (lm-α2) protein results in merosin-deficient muscular dystrophy (MDC1A) (Helbling-Leclerc et al., 1995; Sframeli et al., 2017; Yurchenco et al., 2017). This congenital muscular dystrophy (CMD) results primarily in skeletal muscle damage, but patients often exhibit a broad spectrum of neuroanatomical defects including white matter abnormalities, cerebellar cysts and brainstem (midbrain, pons and medulla) hypoplasia (Philpot et al., 1999; Mercuri et al., 1999). However, the specific functions of lm-α2, particularly in the developing CNS, that lead to these brain abnormalities in MDC1A are unknown.

A further set of clinical symptoms seen in these patients includes neurological deficits in executive functions, intellectual disability and attention deficit hyperactive disorder (ADHD) (Philpot et al., 1999; Mercuri et al., 1999; Ricotti et al., 2016; Jones et al., 2001). This phenotype highlights a possible involvement of the ventral domain of the midbrain, consisting of dopaminergic (mDA) neurons that can be subdivided into two main nuclei, the substantia nigra pars compacta (SNc) and the ventral tegmental area (VTA). SNc mDA neurons are generated first, project largely to the striatum and contribute to the control of voluntary movement, with the selective death of these neurons being the pathological hallmark of Parkinson's disease (Alexander, 2004). In contrast, later-born VTA mDA neurons innervate the hippocampus and the prefrontal cortex (PFC), regulating a range of cognitive functions (Morales and Margolis, 2017). A dopamine imbalance in the VTA mDA neurons has been implicated in the aetiology of ADHD, obsessive-compulsive disorder, addiction and schizophrenia (Blum et al., 2008; Grace, 2016; Nutt et al., 2015).

In this study, we explored the role of lm-α2 protein in NSC development, focussing on the hypothesis that mutations in the *LAMA2* gene disrupt mDA neurogenesis, resulting in a dopamine imbalance that might contribute to some of the neuropsychiatric deficits found in CMD patients. We first confirmed the expression of lm-α2 in the human embryonic ventral midbrain (VM) during mDA neurogenesis. We then utilised a human embryonic stem cell (hESC) model of mDA differentiation to define a functional role for lm-α2 in mDA progenitor proliferation and survival. We confirmed our findings *in vivo* using a lm-α2 null transgenic mouse model. Our findings show that lm-α2 regulates NSC behaviour by controlling the survival of mDA progenitors and their timely differentiation into neurons. In the absence of lm-α2, mDA progenitors are prematurely depleted, resulting in a reduction in the number of late-born mDA neurons in the VTA.

RESULTS

Lm-α2 is present in the developing human VM surrounding mDA progenitors

Using immunohistochemistry (IHC), chain-specific laminin expression in the mesencephalon of human embryos at 6-10 post-conception weeks (pcw) revealed the early embryo (6 pcw) to be

[1]MRC Centre of Regenerative Medicine, University of Edinburgh, Edinburgh EH16 4UU, UK. [2]Departments of Biochemistry and Neurology, School of Medicine and Biomedical Sciences, University at Buffalo, Buffalo, NY 14203, USA. [3]Laboratory of Molecular Neurobiology, Department of Medical Biochemistry and Biophysics, Karolinska Institutet, Stockholm 17177, Sweden.

*Author for correspondence (max.ahmed@ed.ac.uk)

M.A., 0000-0001-8539-7462

Received 11 October 2018; Accepted 24 July 2019

Development (2019) 146, dev172668. doi:10.1242/dev.172668

rich in lm-α2 (Fig. 1). The VM was immunopositive for lm-α2 throughout the entire apico–basal axis surrounding a population of rapidly dividing (Ki67$^+$) mDA progenitors. Analysis of a previously published single-cell RNA sequencing (scRNA-seq) study of the human VM between 6 and11 pcw suggests that pericytes are a potential contributing cell source and could potentially secrete this laminin into the interstitial space (Fig. 1) (La Manno et al., 2016). A developmental time-course analysis revealed that protein expression diminished over time; by 10 pcw, lm-α2 expression was largely absent from the human VM. Similarly, in the mouse VM, lm-α2 protein expression rapidly diminished after E10.5 with little or no detectable lm-α2 at E14.5 (Fig. S1). The loss of interstitial lm-α2 expression correlated with the loss of proliferating mDA progenitors, suggesting a potential role for lm-α2 in supporting self-renewal. Examination of the spatiotemporal expression patterns of the remaining four lm-α chains revealed the basal laminae of the blood vessels within the VM to be rich in lm-α4 (Fig. S1), consistent with scRNA-seq data showing expression to be greatest in endothelial cells and pericytes. Expression of lm-α1 was most pronounced in the basement membrane lining the basal surface of the neural tube, whereas lm-α5 could be seen on the ventricular surface and interspersed around the cells of the VM. This finding is again consistent with scRNA-seq data showing expression of these laminin genes in radial glial cells (Rgls, whose processes span the two surfaces of the developing mesencephalon) and progenitors (Fig. S1). Lm-α3 protein and mRNA expression were absent in the midbrain floor plate, underlining the specificity of the different laminin expression patterns.

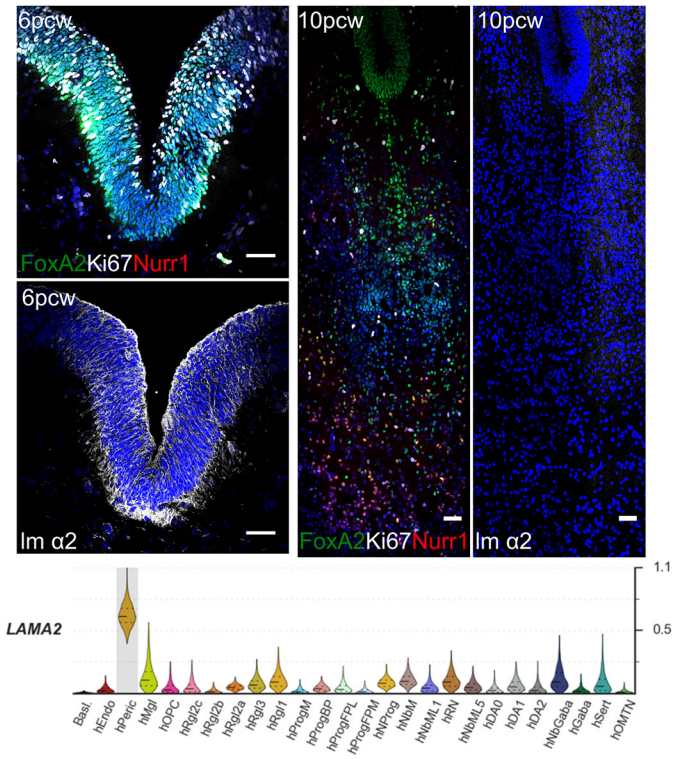

Fig. 1. Lm-α2 expression in human VM at 6 and 10 pcw. Lm-α2 expression (antibody, C13065) is enriched in human VM at 6 pcw, when it is composed of Ki67$^+$ FoxA2$^+$ progenitors. Expression diminishes by 10 pcw when the VM contains few Ki67$^+$ cells and postmitotic Nurr1$^+$ mDA neurons are established. scRNA-seq of human VM suggests that pericytes (hPeric) are the principal source of lm-α2. Right axis shows absolute molecule counts. Scale bars: 50 µm in all images.

Lm211 regulates the balance between proliferation and differentiation in a concentration-dependent manner and controls the survival of human mDA progenitors

To assess the functional role of lm-α2, a hESC model of mDA differentiation was established (Fig. S2) using a previously published protocol capable of yielding mDA neurons positive for a range of markers such as tyrosine hydroxylase (TH), Nurr1, DOPA decarboxylase (DDC), Pbx1a, Girk2 and calbindin (Fig. S2) (Kirkeby et al., 2012). Day 14 VM progenitors that are positive for FoxA2, Lmx1a and Otx2 (Fig. S2), analogous to mDA progenitors *in vivo* at 6 pcw, were incubated with the recombinant version of the lm-α2-containing trimeric protein lm211 at concentrations ranging from 0.5 to 12 µg ml^{-1} for a period of 14 days. The thymidine analogue 5-ethynyl-2′-deoxyuridine (EdU) was administered prior to fixation to label proliferating cells. Cultures were stained for TH, which marks mDA neurons. Increasing the concentration of lm211 increased the number of mDA progenitors that were EdU$^+$, with a concomitant reduction in the number of TH$^+$ mDA neurons (Fig. 2A-C).

Focussing on two concentrations favouring proliferation (4 µg ml^{-1}) and differentiation (1 µg ml^{-1}), the differentiation dynamics were interrogated further. Cultures were fixed at days 21, 28 and 35 and were examined for proliferation (EdU), differentiation (Nurr1 and TH) and cell death (active caspase 3, aC3). No differences were detected at day 21 between the two conditions; however, the lm211-rich environment (4 µg ml^{-1}) sustained cells in a proliferative state (Fig. 2D) and consequently delayed differentiation, resulting in fewer Nurr1$^+$ postmitotic neuroblasts (Fig. 2E) and TH$^+$ neurons (Fig. 2F) being detected at days 28 and 35 compared with the lm211-poor condition (1 µg ml^{-1}). Although the number of apoptotic cells increased over the duration of the culture, no significant difference was detected between apoptotic cell numbers at the two lm211 concentrations (Fig. 2G).

Having shown a role for lm211 in promoting VM progenitor proliferation, we next determined whether this property was specific to the lm-α2 isoform by treating the cultures with three other laminin isoforms (lm111, lm411 and lm511) at the previously identified concentrations (1 and 4 µg ml^{-1}). Rates of proliferation of mDA progenitors were the same for all laminin isoforms, with no significant difference detected in EdU labelling at either concentration (Fig. S3A,B,D). Similarly, no effect on the number of TH$^+$ cells was detected at high concentrations of lm-α isoforms (Fig. S3E). Surprisingly, however, a significant increase in the number of TH$^+$ neurons was detected for lm211 at low concentration, compared with the other three isoforms (Fig. S3C). We therefore determined whether this increase in TH$^+$ neurons in response to low concentrations of lm211 was due to enhanced differentiation or survival by examining aC3 immunoreactivity (a marker of apoptosis) for the four different laminin isoforms. Significantly fewer aC3$^+$ cells were seen after lm211 treatment (Fig. S3F), suggesting that the increase in the number of mDA neurons is a result of improved cell survival. Taken together, these results suggest that lm211 has distinct concentration-dependent effects, with a laminin-rich environment supporting proliferation and expansion of the progenitor pool irrespective of isoform, whereas low concentrations of lm-α2-containing isoform promote survival of mDA lineage cells.

Interaction of Lm211 and human mDA progenitors is mediated by distinct receptor engagement

To identify the cell surface receptors responsible for the different effects of lm-α2 on mDA progenitors, we used a functional blocking

Development (2019) 146, dev172668. doi:10.1242/dev.172668

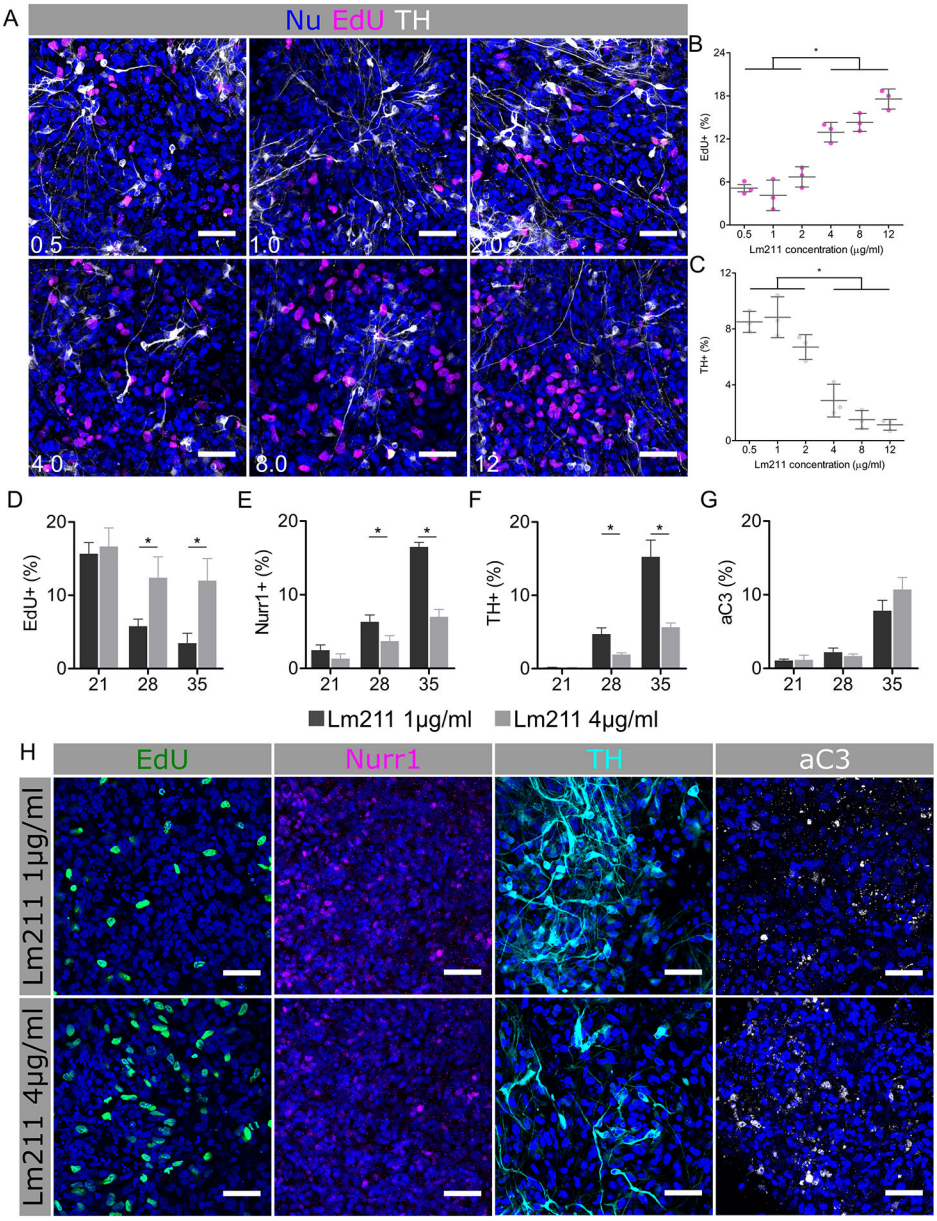

Fig. 2. Lm211 regulates proliferation and differentiation in a concentration-dependent manner. (A) Immunostaining of day 28 hESC-derived mDA cultures treated with lm211 over a concentration range of 0.5-12 μg ml^{-1}. (B,C) Quantification of EdU (B) and TH (C) staining shows a significant increase in proliferating (EdU^{+}) cells at lm211 concentrations of over 4 μg ml^{-1}. The increase is associated with a reduction in TH^{+} mDA neurons (one-way ANOVA with Tukey's post hoc test; P<0.0001, n=3). (D-G) Time series examining proliferation (D), differentiation (E,F) and survival (G) at days 21, 28 and 35 of culture at two different lm211 concentrations. mDA progenitors remain EdU^{+} at day 28 and 35 in the lm211-rich (4 μg ml^{-1}) environment, resulting in significant reduction in the number of postmitotic mDA neuroblasts (Nurr1) and neurons (TH). There were no significant differences in aC3 staining between the two lm211 concentrations. Unpaired two-tailed t-test; *P<0.0001, n=3. (H) Representative images of day 35 cultures following lm211 treatment. Scale bars: 50 μm in all images.

antibody approach. As the laminin-rich environment maintains cells in a proliferative state irrespective of isoform, we speculated that the integrin family of receptors were involved. Three principal laminin-binding integrins (α3β1, α6β1 and α7β1) have been identified. All were expressed in the human VM; scRNA-seq analysis showed that human Rgls and midline progenitors express significant levels of integrin α6 and detectable levels of integrins α7 and β1 (Fig. S4). We further confirmed the presence of these three integrin subunits via immunostaining of hESC-derived mDA progenitors (Fig. S4). Blocking the β1 integrin subunit resulted in complete loss of adhesion and cell detachment (data not shown) whereas blocking the individual α-subunits had a negligible effect on mDA progenitor proliferation (Fig. 3B). As the integrin α-subunits might functionally compensate for each other, we next blocked pairwise combinations of α-subunits. Blocking integrin α3 had no discernible effect, but the combined blockade of both integrins α6 and α7, in the presence of 4 μg ml^{-1} lm211, resulted in loss of the lm211-driven increase in EdU^{+} mDA progenitors and an increase in the number of TH^{+} mDA neurons (Fig. 3B,C). We further confirmed the role of integrins α6 and α7 in mediating the proliferative response by blocking both receptors in the presence of lm111, lm411 and lm511 at 4 μg ml^{-1} and successfully reversing the increase in proliferating mDA progenitors (Fig. S5).

Because the increased cell survival of hESC-derived mDA lineage cells (Fig. S3C,G) was specific to low concentrations of lm-α2, we speculated that dystroglycan (a high-affinity lm-α2 receptor enriched in the floor plate, the point of origin of mDA neurons) could be mediating the effect (Anderson et al., 2007; Schofield et al., 1995; Wright et al., 2012). We confirmed the expression of dystroglycan in human VM via immunostaining and also in the scRNA-seq dataset, in which it is expressed at significant levels in human Rgls (Fig. S4). Blocking dystroglycan with a targeted antibody (IIH6C4) *in vitro* reversed the laminin isoform-specific increase in TH^{+} neurons seen using low concentrations of lm211 to levels comparable to those seen for lm111 (Fig. 3D-F). When we administered the antibody without any exogenous lm211, we did not observe any significant differences in TH^{+} cells, confirming the laminin-specific nature of the interaction (Fig. S5).

Development (2019) 146, dev172668. doi:10.1242/dev.172668

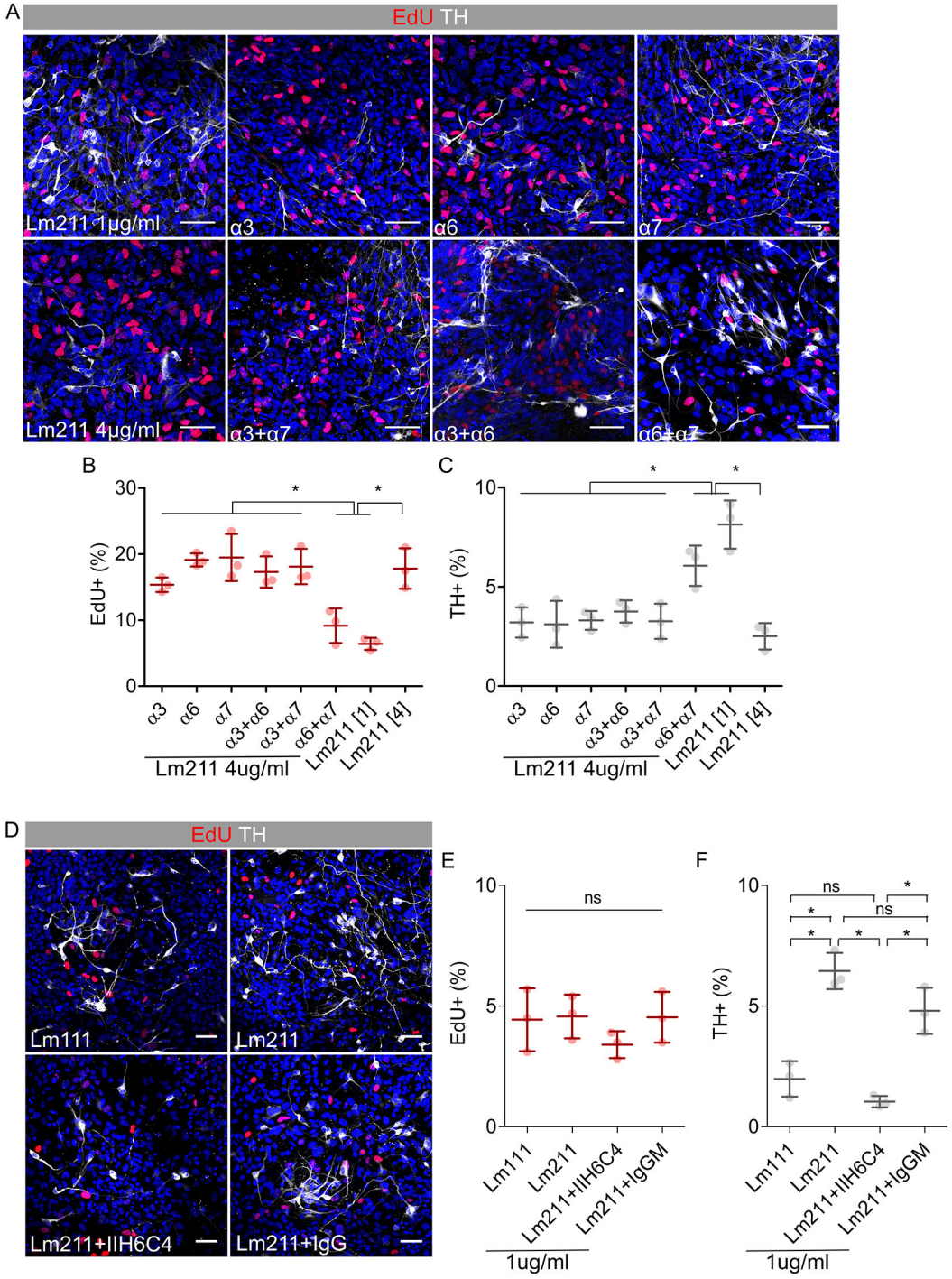

Fig. 3. Concentration-dependent effects of lm211 are mediated by distinct receptor engagement. (A) Immunostaining of day 28 cultures treated with lm211 (4 µg ml^{-1}) in combination with integrin blocking antibodies and a control condition of lm211 (1 µg ml^{-1}). (B,C) Quantification of proliferation (B) and differentiation (C) following blocking of integrin α-subunit demonstrates that blocking both integrins α6 and α7 reverses the effect of the lm211-rich environment. (D) Images of day 28 cultures treated with laminin isoforms (1 µg ml^{-1}) and dystroglycan blocking antibody or isotype control. (E,F) Quantification of proliferation (E) and differentiation (F) demonstrates that blockade of dystroglycan reverses the gain in mDA neurons seen in response to treatment with lm211 compared with lm111 without effecting proliferation. Unpaired two-tailed *t*-test; **P*<0.0001, *n*=3. Scale bars: 50 µm in all images.

Loss of progenitors and premature differentiation results in reduced number of neurons in the VM of *Lama2* null mice

Together, results using human cells and tissue suggest the hypothesis that the fall in lm-α2 expression levels in the human VM between 6 and 10 pcw controls VM NSC cell cycle exit and mDA neuron differentiation, with lower concentrations of lm-α2 supporting cell survival. To confirm that lm-α2 is such an instructive component of the niche *in vivo*, we examined the VM of lm-α2 null mouse embryos during mDA neurogenesis at embryonic (E) day 10.5-14.5, corresponding to 6-10 pcw in humans. We first confirmed that the lm-α2 null embryos do not express lm-α2 (Fig. S6).

Development (2019) 146, dev172668. doi:10.1242/dev.172668

Our hypothesis predicts that in the absence of lm-α2 there would be fewer mDA progenitors and more neurons as a result of the loss of the proliferative effect of this laminin, resulting in premature differentiation. This was confirmed; the *Lama2*$^{-/-}$ embryos were smaller than wild-type (WT) littermate controls and the VM domain, demarcated by FoxA2 expression, consisted of significantly fewer cells (Fig. S7A-D). Premature differentiation at E10.5 could be detected in the *Lama2*$^{-/-}$ embryos, as evidenced by increased numbers of Nurr1^{+} and TH^{+} cells at this age, with a concomitant reduction in proliferating VM progenitors (double Ki67^{+} and FoxA2^{+} cells) (Fig. 4A-D). Nascent mDA neurons were seen not only in the marginal zone along the basal surface of the VM but also in ectopic positions at the ventricular surface of the *Lama2*$^{-/-}$ VM (Fig. S8), a region where the high concentration of lm-α2 would normally prevent differentiation.

To exclude the possibility that the observed reduction in size of the VM resulted from patterning defects rather than changes in proliferation, we examined the position of cells expressing FoxA2, Lmx1a or Corin and calculated the area of their domains, normalised to the area of the ventricle. No significant difference in position or domain sizes was seen at E10.5 or E12.5 (Fig. S7), suggesting that patterning is unaffected in the mutant embryos. We also examined the expression patterns of *Nkx6-1* and *Wnt1* in WT and mutant embryos at E12.5 and found no differences (Fig. S7H,I). We did, however, note a slight delay in the lateral expansion and medial inhibition of Shh expression, with low levels of Shh in the mutant basal plate compared with the controls (Fig. S7I). This finding is in agreement with both the known function of Shh to control expansion of the VM (Ishibashi and McMahon, 2002; Britto et al., 2002) and with our findings of a decreased number of FoxA2^{+} cells (Fig. S7K), impaired growth and reduced proliferation in the VM.

Our original hypothesis also predicts increased levels of apoptosis caused by the loss of the survival-promoting effect of low concentrations of lm-α2. Again, this was confirmed; by E12.5, numerous active aC3^{+} cells were found along the border of the ventricular zone and intermediate zone that separates progenitors from postmitotic neuroblasts, suggesting that apoptosis takes place during cell cycle exit (Fig. 4E). Quantification revealed a near twofold increase in aC3^{+} cells and fewer FoxA2^{+} progenitors (double FoxA2^{+} and KI67^{+} cells) in the VM (Fig. 4F,J).

Ectopic TH+ neurons were once again detected at the ventricular surface of the mutant VM at E12.5 (Fig. S8). However, in contrast to the situation at E10.5, by E12.5 the intermediate and marginal zone of the *Lama2*$^{-/-}$ embryos contained fewer Nurr1^{+} and TH^{+} cells (Fig. 4H,I). To determine the cause of this reduction in neuron number, we next examined the expression of the proneural gene encoding neurogenin 2 (Ngn2) in Lmx1a^{+} mDA progenitors (Kele et al., 2006). Although these experiments confirmed the reduction of midbrain floor plate mDA progenitors (identified as Lmx1a^{+}) we found no significant difference in the subset of progenitors undergoing neurogenesis (identified as Ngn2^{+}) in *Lama2*$^{-/-}$ embryos (Fig. 4L). Consequently, we conclude that the proportion of progenitors undergoing neurogenesis is greater in the mutant embryos, leading to accelerated differentiation and depletion of the progenitor pool. To test this directly, we injected pregnant mice subcutaneously with EdU at E11.5 and dissected the embryos 24 h later at E12.5. We then quantified the number of dividing cells (EdU^{+}) that had exited cell cycle and were positive for the postmitotic marker Nurr1. Confirming our previous results, we found a significant increase in neurogenesis, with a 26% increase in the number of cells positive for both EdU and Nurr1 in the mutant embryos compared with WT littermate controls. Meanwhile, there was a significant decrease in the number of Lmx1a^{+} EdU^{+} cells that were Nurr1^{-} (i.e. mDA progenitors that were still in cell cycle). Consistent with this, by E14.5, there were significantly fewer TH^{+} neurons in the mutant embryos than in the WT littermate controls (Fig. S9).

To determine whether these effects are restricted to the mDA lineage, we next examined non-mDA neurons in the VM. Brn3a is a marker of neurons within the red nucleus, immediately lateral to the mDA neuron domain. The number of Brn3a^{+} neurons in *Lama2*$^{-/-}$ mutants was significantly reduced compared with WT littermate controls at E14.5 (Fig. S10), indicating that basal plate neurogenesis was also impaired.

Lm-α2 null mice have fewer calbindin^{+} mDA VTA neurons

Birth-dating experiments have demonstrated that mDA neurons are born sequentially, with more lateral mDA neurons that project to the striatum born first and the medial mDA neurons projecting to the PFC born later in development (Bayer et al., 1995; Bye et al., 2012). To examine how the altered differentiation dynamics in the mutant embryos affects the distribution and subtype composition of mDA neurons in the postnatal brain, we examined the expression of Girk2 and calbindin, markers expressed predominantly in the lateral SNc mDA neurons and the medial VTA mDA neurons, respectively, at postnatal (P) day 15. Both subpopulations of TH^{+} mDA neurons can be identified in the VM of both WT and mutant brains, with the calbindin^{+}/TH^{+} cells clustered around the ventral midline and the Girk2^{+}/TH^{+} cells distributed more laterally (Fig. 5A). A small subsection of mDA neurons expressing both Girk2 and calbindin were found largely restricted to the dorsolateral VTA in the transition zone between the SNc and VTA. The *Lama2*$^{-/-}$ brains were found to be smaller at P15 (Fig. S11) and to have fewer TH^{+} mDA neurons in the midbrain compared with WT littermate controls (Fig. 5B). The loss of neurons was particularly apparent in the mediocaudal VM (Fig. S12), suggesting that the later-born medial mDA neurons were preferentially depleted in the mutant mice. Quantifying Girk2 and calbindin expression confirmed this, revealing a reduction in the number of TH^{+} calbindin^{+} (later-born) mDA neurons and no significant decrease in the number of Girk2^{+} TH^{+} (early-born) mDA neurons (Fig. 5C,D). As expected, quantification of the ratio of TH^{+} mDA neurons that are either Girk2 or calbindin^{+} in the mutant brains revealed proportionately more Girk2^{+} and fewer calbindin^{+} mDA neurons (Fig. 5E). These results suggest that premature depletion of the mDA progenitor pool, caused by a smaller progenitor domain combined with accelerated differentiation and increased apoptosis, leads to loss of late-born calbindin^{+} mDA neurons and thus creates an imbalance between these two populations of dopaminergic neurons in the VM of *Lama2*$^{-/-}$ brains.

DISCUSSION

In this study, we describe the expression and distribution of laminin isoforms in mouse and human VM and identify a dual functional role for one of these, lm-α2, in controlling cell cycle exit and survival in the mDA neuron lineage. We propose a model whereby the lm-α2-rich environment, found early in development, sustains VM progenitor proliferation via an integrin-dependent pathway. As lm-α2 expression diminishes, cells are able to exit from the cell cycle and differentiate, with low levels of lm-α2 promoting the survival of progenitors through dystroglycan receptors. In mutant *Lama2*$^{-/-}$ mice, the loss of lm-α2 protein results in a smaller mDA progenitor pool that is subsequently depleted by a combination of increased cell death and premature differentiation, leading to a defect in late-generated mDA neurons of the VTA subtype.

Development (2019) 146, dev172668. doi:10.1242/dev.172668

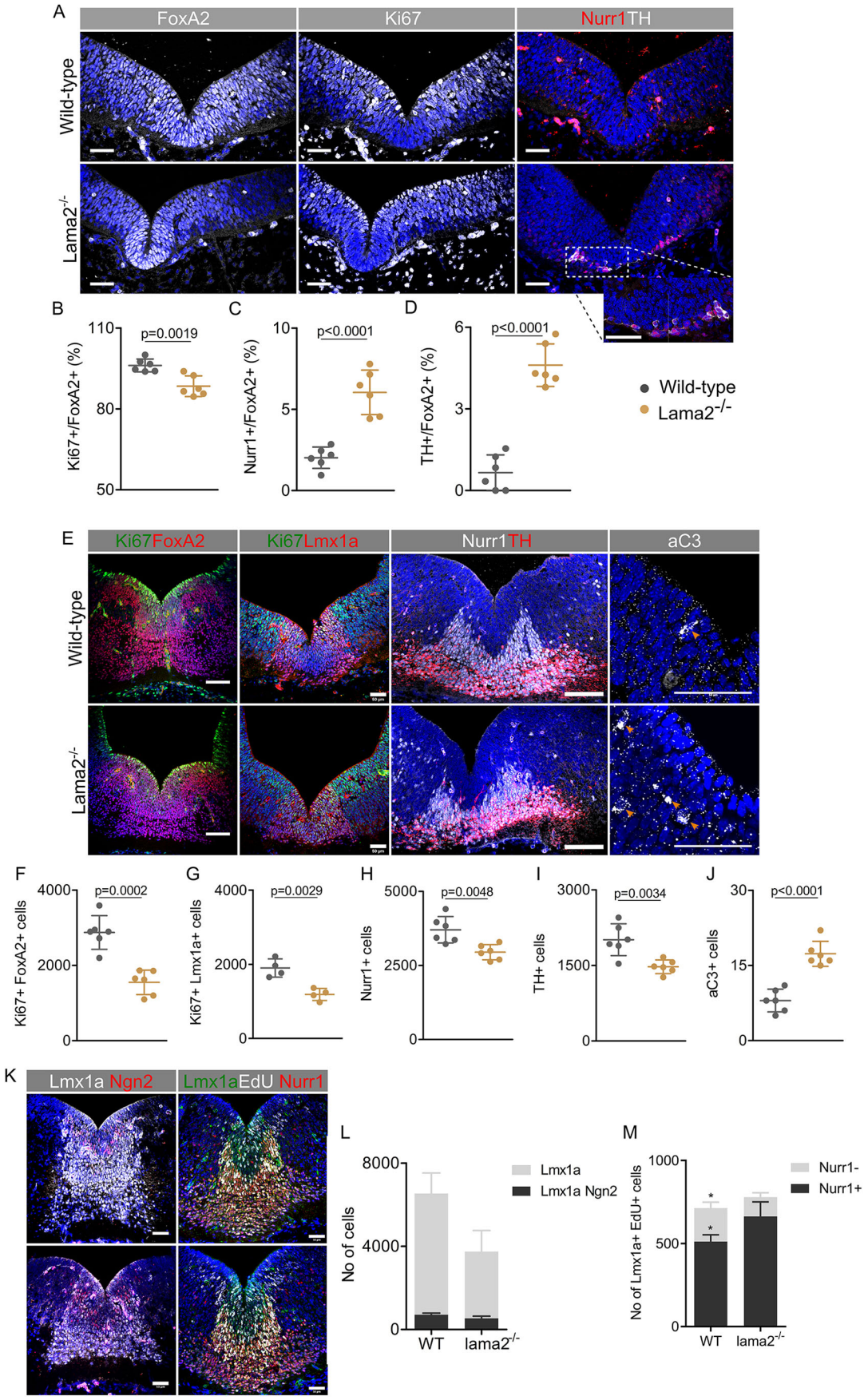

Fig. 4. See next page for legend.

Development (2019) 146, dev172668. doi:10.1242/dev.172668

Fig. 4. Lm-α2 null VM is reduced in size with fewer cells and exhibits premature differentiation and depletion of the progenitor pool. Representative images and quantification of WT and mutant VMs at (A-D) E10.5 and (E-M) E12.5. (A) At E10.5, mutant embryos display a smaller ventral domain, as indicated by FoxA2 staining. (B-D) Quantification shows that fewer FoxA2$^+$ cells are Ki67$^+$ in the *Lama2*$^{-/-}$ embryo (B) but there are increased numbers of postmitotic mDA neuroblasts (Nurr1$^+$; C) and mDA neurons (TH$^+$; D). (E-J) By E12.5, there remain fewer proliferating FoxA2$^+$ cells (F) and Lmx1a$^+$ cells (G) in the VM of mutant embryos. (H-J) The intermediate and marginal zones of the mutant VM contain fewer Nurr1$^+$ (H) and TH$^+$ (I) cells, whereas there is an increase in apoptotic (aC3$^+$) cells (J) at the ventricular zone and intermediate zone border in the absence of lm-α2. (K-M) Although there is a reduction in the number of Lmx1a$^+$ mDA progenitors, the number of Lmx1a$^+$ Ngn2$^+$ cells remains the same (L), resulting in a greater proportion of progenitors undergoing neurogenesis [12.51±0.89% (WT) versus 20.73±3.49% (*Lama2*$^{-/-}$)] in the mutant embryos. (M) EdU labelling confirmed this with a significant increase in the number of EdU$^+$ Nurr1$^+$ cells in the mutant embryos [512±41 (WT) versus 663±88 (*Lama2*$^{-/-}$)], whereas there was a significant decrease in the number of Lmx1a$^+$ EdU$^+$ cells that are Nurr1$^-$ [201±35 (WT) versus 116±26 (*Lama2*$^{-/-}$)]. Unpaired two-tailed *t*-test; **P*<0.01, *n*=4-6. Scale bars: 50 µm in all images.

Previous studies examining laminin expression in the brain describe the murine neocortex as being rich in lm-α2 and lm-α4, with expression greatest at the ventricular surface (Fietz et al., 2012; Lathia et al., 2007). Moreover, the subventricular zone, one of two adult stem cell niches in the CNS, was found to be a laminin-rich environment compared with neighbouring non-neurogenic regions, suggesting that laminins play a role in regulating NSC self-renewal (Kazanis et al., 2010). Consistent with this, we found the presence of high levels of interstitial lm-α2 in the early human embryo during a period of rapid growth, after which levels decline. Three other laminin isoforms (lm-α1, lm-α4 and lm-α5) were largely restricted to the basal lamina. Together, our immunostaining and analysis of a previously published scRNA-seq dataset reveal laminin expression to be highly specific and dynamically regulated over the course of development.

Several independent studies have implicated laminin–integrin interactions in the control of NSC proliferation in both the embryonic cortex and adult stem cell niches (Shen et al., 2008; Loulier et al., 2009; Tan et al., 2016; Nascimento et al., 2018). Additionally, in pathological conditions characterised by rapid proliferation, such as glioblastoma multiforme (GBM), the cellular niche has been described as rich in lm-α2 whereas the glioblastoma stem-like cells that drive tumour growth are enriched with integrins α6 and α7 (Lathia et al., 2012, 2010; Haas et al., 2017). Disruption of laminin–integrin interactions in GBM significantly impairs tumour growth (Lathia et al., 2012, 2010; Haas et al., 2017). Given our results showing that the expression of lm-α2 in mDA progenitors maintains cells in a proliferative state, it would be interesting to test the hypothesis that a common mechanism underpins laminin–integrin interaction-driven NSC proliferation

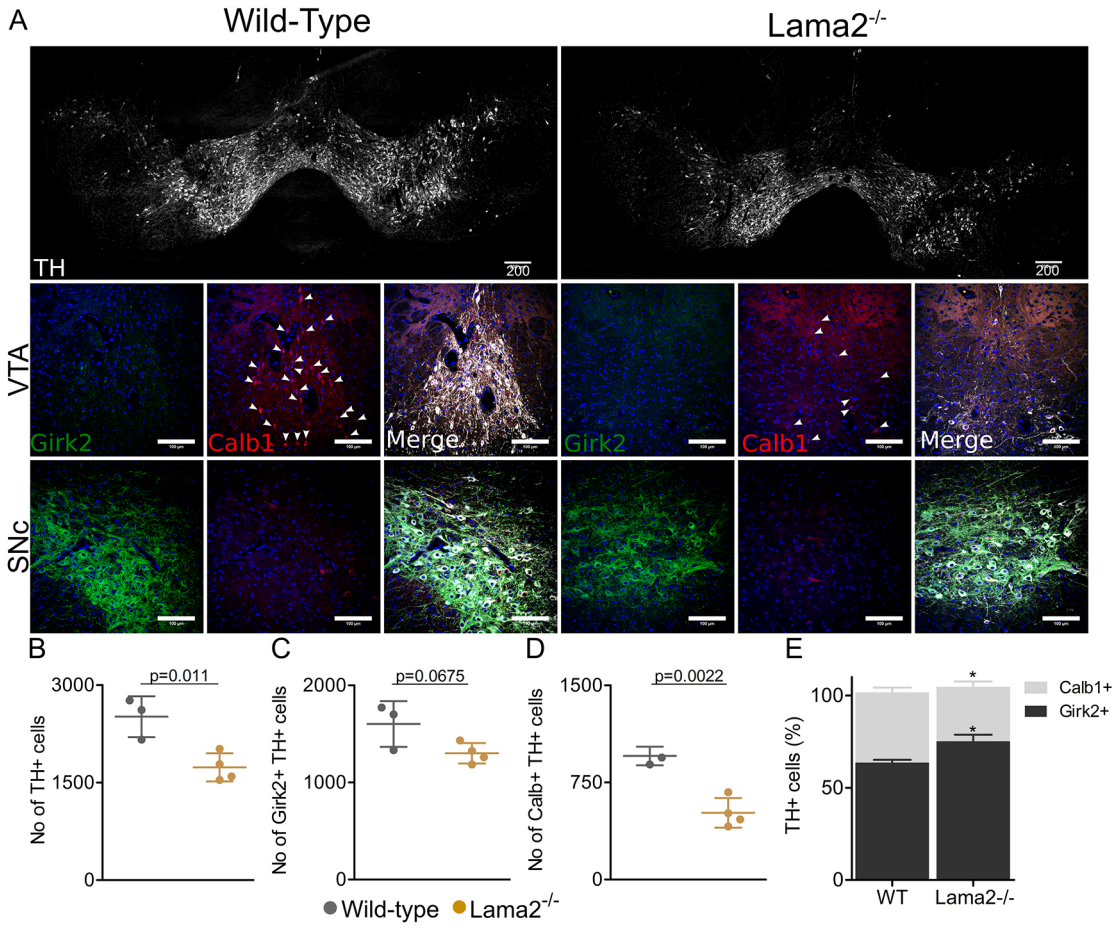

Fig. 5. The midbrain of lm-α2 null brains contains fewer late-born calbindin$^+$ mDA neurons of the VTA. (A-E) Immunostaining of postnatal brains (P15) of WT and mutant mice (A) shows fewer TH$^+$ mDA neurons in *Lama2*$^{-/-}$ brains (B). In quantifying mDA subtype, there is a modest reduction in the number of Girk2$^+$ mDA neurons (C) but a dramatic loss in calbindin$^+$ mDA neurons (D) located medially in the VM. In normalising for the number of mDA neurons (E), there is a significant increase (*P*=0.0033) in the proportion of Girk2$^+$ TH$^+$ mDA neurons in the mutant mice concomitant with a reduction (*P*=0.0105) in calbindin$^+$ TH$^+$ mDA neurons. Unpaired two-tailed *t*-test; *n*=3 (WT), *n*=4 (KO). Scale bars: 100 µm in all images unless stated.

Development (2019) 146, dev172668. doi:10.1242/dev.172668

in embryonic, adult and pathological conditions. Identifying downstream mechanisms as well as positive and negative regulators of laminin expression could be important, not only to control proliferation in cancer but also in a regenerative context, offering the potential to counteract the age-dependent decline in NSC self-renewal.

Over the course of development, laminin expression diminishes and is restricted to the ventricular zone, limiting the cells it can interact with to those rapidly dividing progenitors juxtaposed to the surface of the ventricle. The interaction with lm-α2 in this region prevents exit from the cell cycle and differentiation. As predicted from this hypothesis, precocious mDA neurons can be seen at both the basal surface and ectopically at the ventricular surface in the complete absence of lm-α2. An increase in the number of apoptotic cells in the interface between the ventricular and intermediate zone can also been seen, reflecting the requirement for lower concentrations of lm-α2 to maintain the survival of newly postmitotic cells in this region. A previous study showed that lm-α5-driven yes-associated protein (YAP) activation promotes survival of mDA neurons in the marginal zone (Zhang et al., 2017), but at a later differentiation stage than that described in this study. Interestingly, lm-α2 has also been reported to activate YAP and further upregulate the expression of laminin receptors such as integrins and dystroglycan in Schwann cells (Poitelon et al., 2016), suggesting a possible interaction between these two laminin-activated pathways and a general role for laminins in controlling cell survival at different developmental stages along the same lineage. Indeed, it is perfectly feasible that the lm511 present in VM is compensating for loss of lm211, masking the extent of the phenotype.

We have previously shown that the principal laminin receptor, integrin β1, is capable of regulating both NSC self-renewal and differentiation in the chick midbrain via distinct mechanisms (Long et al., 2016). Meanwhile, the relative abundance of the laminin protein has been shown to control the balance between quiescence and activation in epidermal stem cells (Morgner et al., 2015). Our present results extend these prior studies by showing that a concentration-dependent effect of lm-α2 controls the proliferation and survival of human progenitors, at least in part, by sequential receptor engagement with integrins and dystroglycan. It is interesting that a similar interplay between the two receptors has been identified in laminin-mediated pancreatic β-cell development (Jiang et al., 2001). Moreover, αβ-integrins and dystroglycan have been shown to act sequentially during Schwann cell development in the peripheral nervous system, activating different signalling pathways during axonal sorting (Berti et al., 2011). In agreement with these previously published studies, the data presented here suggest that the two laminin receptors are responsible for distinct steps during mDA development. How lm211 is able to regulate these specific processes in a concentration-dependent manner remains an open question. One possible explanation could lie in receptor affinities. Previously published solid-phase binding assays of lm211 with dystroglycan and a number of α-integrins demonstrated that the dystroglycan interaction is an order of magnitude greater than interaction with integrins (Nishiuchi et al., 2003; Talts et al., 1999) and so is likely to be favoured at the lower laminin concentrations found later in the developmental process.

Mutations affecting lm-α2, dystroglycan and more rarely integrin α7 result in CMD, a clinically and genetically heterogeneous group of disorders primarily affecting muscle and brain. Neurological deficits that include structural malformations and cognitive impairment are most abundant in patients carrying mutations affecting dystroglycan (Bertini et al., 2011; Clement et al., 2008). However, a number of patients carrying a *LAMA2* mutation also report neurological abnormalities, including brainstem hypoplasia (Philpot et al., 1999; Mercuri et al., 1999). In the lm-α2 null embryos described in this study, we found the VM to be significantly reduced in size, probably caused by impairment of proliferation, premature differentiation and increased cell death resulting in depletion of the progenitor pool. This phenotype is reminiscent of integrin β1 mutant mice in which cerebellar granule cell precursors cease proliferating and differentiate prematurely (Blaess et al., 2004). Interestingly, impaired Shh signalling contributes to premature differentiation in integrin β1 mutant mice following disruption of the integrin–laminin–Shh complex (Blaess et al., 2004). Moreover, Shh–proteoglycan interactions were shown to be necessary for regulating proliferation but dispensable for tissue patterning (Chan et al., 2009). We found a defect in proliferation but with correct patterning and a subtle delay in *Shh* expression in lm-α2 null embryos, so a contribution of Shh signalling to the proliferation phenotype cannot be excluded.

A well-established consequence of premature differentiation and depletion of the progenitor pool is loss of later-born neurons (Lai et al., 2008; Hatakeyama et al., 2004; Bedford et al., 2005). In accordance, we found a disruption of mDA neuron subtype composition, with a reduction in later-born calbindin^{+} mDA neurons of the VTA. The mDA neurons of the VTA project to the caudal brainstem, hippocampus and PFC and play an important role in a number of processes, including cognition, motivation and attention-related behaviour. Indeed, a subset of these late-born mDA neurons project almost exclusively to the GABAergic interneurons of the PFC and regulate perseveration-like behaviour (Kabanova et al., 2015). This loss of late-born neurons could contribute to the cognitive defects described in the few published reports of behavioural and psychiatric problems in MDC1A patients. Of potentially more importance, however, is the possibility that abnormalities in the laminin–dystroglycan–dystrophin pathway caused by dystrophin mutations in Duchenne muscular dystrophy (DMD) patients might, by altering mDA neuron production, contribute to the high prevalence of ADHD and autism spectrum disorder (ASD) described in a recent study of 130 DMD patients (Ricotti et al., 2016). In keeping with this, a separate study reported a reduction in $GABA_A$ receptor clustering in the PFC (a target of late-born mDA neurons) of 14 DMD patients (Suzuki et al., 2017). Given the roles we have ascribed to lm-α2, a more thorough behavioural and psychiatric analysis of MDC1A patients would be of great value and provide some support for the notion that a dopamine imbalance underpins the behavioural deficits observed in muscular dystrophies.

MATERIALS AND METHODS

Human and mouse tissue processing

OCT Tissue-Tek-embedded human foetal tissue (5-10 pcw) was obtained with consent from the MRC-Wellcome Trust Human Developmental Biology Resource (HDBR). Sequential coronal sections covering the length of the mesencephalon were collected on superfrost glass slides (ThermoFisher) using a cryostat (ThermoFisher).

All mouse experiments were conducted following the procedures approved by Roswell Park Institute Animal Care and Use Committee (UB1188M, UB1194M and UB1196R). The protocols follow the guidelines of the 'Guide for the Care and Use of Laboratory Animals' (National Research Council, National Academy Press, Washington D.C., 1996). All animals used in this work were congenic into the C57/BL6N background and genotyping of *Lama2* mutant mice was done by PCR of tail genomic DNA. Briefly, PCRs were carried out for 45 s at 95°C, 45 s at 50°C, and 60 s at 72°C for 30 cycles. The primers used were 5′-CCCGTGATATTGCTGAAG-3′, 5′-CCTCTCCATTTTCTAAAG-3′ and

Development (2019) 146, dev172668. doi:10.1242/dev.172668

5′-CAGGTGTTCCAGATTGCC-3′. The *Lama2* mutant used in this study was the dy3k mutant comprising a complete knockout of the lm-α2 protein (Miyagoe et al., 1997).

To obtain embryos, matings were set late in the evening and plugs checked the next morning before 9 a.m., with those that were positive designated as E0.5. At E10.5, E12.5 and E14.5, pregnant mice were sacrificed. E10.5 whole-mount embryos and the dissected heads of E12.5 and E14.5 embryos were fixed in 4% PFA overnight at 4°C.

For the EdU labelling studies, pregnant mice were subcutaneously injected with 50 mg kg^{-1} of EdU (Sigma 900584) at E11.5. Embryos were dissected 24 h later at E12.5, washed in PBS (3×5 min) and incubated in 15% sucrose (Sigma) in PBS at 4°C overnight. The embryos were then placed in embedding solution consisting of 15% sucrose and 7% gelatin (Sigma) in PBS at 37°C for a period of 2 h. Finally, the embryos were placed in moulds, orientated for coronal sections, snap frozen in liquid N_2 and stored at −80°C. Serial sections of 10 µm, spanning the length of the midbrain, were taken from each sample. Two embryos from two or three different litters were analysed for each time point (n=4-6). Individual figure captions make clear the number used for each experiment.

In the case of P15 brains, animals were anaesthetised with 20 mg ml^{-1} Avertine (2,2,2-tribromoethanol, Sigma, T48402) and sequentially perfused through the left ventricle with ice-cold 1× PBS and 4% PFA. Next, the brains were dissected and post-fixed in 4% PFA overnight at 4°C, transferred to 30% sucrose for 48 h at 4°C and then snap frozen in liquid N_2. Sections of 20 µm were collected on glass slides. Two brains from two different litters were examined for both mutant and control animals (n=4).

Cell cultures

Undifferentiated RC17 ES cells (passages 23-58; Roslin Cells, hPSC reg #RCe021-A) were maintained in E8 media (A1517001) on plates coated with 1% Geltrex (ThermoFisher, 12760021) and passaged weekly with EDTA (0.5 mM). To start differentiation (day 0), hESC colonies were detached using EDTA (0.5 mM) and placed in untreated 60 mm culture dishes in differentiation medium consisting of DMEM:F12/Neurobasal (1:1), N2 supplement (1:100), B27 supplement (1:50), SB431542 (10 µM, Tocris Biosciences), rhnoggin (100 ng ml^{-1}, R&D), SHH-C24II (200 ng ml^{-1}, R&D) and CHIR99021 (0.9 µM, Tocris Biochem). Medium was changed once on day 2. The resultant embryoid bodies were collected on day 4 and placed on polyornithine (PO)-, fibronectin (Fn)- and laminin-coated plates in medium with reduced N2 (1:200) and B27 (1:100) supplements. Growth and patterning factors were removed on day 9 with the cultures kept in DMEM:F12/Neurobasal (1:1), N2 supplement (1:200) and B27 supplement (1:100). On day 11, the cell clusters were dissociated to single cells with Accutase and re-plated onto dry PO/Fn-coated plates for differentiation in Neurobasal, B27 (1:50), BDNF (20 ng ml^{-1}), GDNF (10 ng ml^{-1}), ascorbic acid (200 µM) and db-cAMP (0.5 mM, Sigma). All culture reagents were from Invitrogen unless otherwise stated.

Experiments were conducted from day 14, where cultures were treated with soluble laminin isoform (BioLamina) or vehicle, with each medium change, for the stated period of time. Medium was changed every third day until fixation in 3.7% PFA for 30 min. Where stated, an EdU pulse was administered for 24 h prior to fixation to identify dividing cells.

Receptor-blocking antibodies or isotype controls were added to the culture medium at 5 µg ml^{-1} (10 µg ml^{-1} for dystroglycan) and refreshed every 3 days with each change of medium. Antibodies used were integrin α3 IA3 (R&D MAB1345-SP), integrin α6 GoH3 (R&D MAB13501), integrin α7 6A11 (LifeSpan Biosciences, LS-C179572), dystroglycan IIH6C4 (Millipore, 05-593), mouse-IgM (ThermoFisher, 02-6800), rat-IgG2a (ThermoFisher, 02-9688) and mouse-IgG1 (ThermoFisher, 02-6100).

Immunofluorescence, microscopy and image quantification

Lists of antibodies used, suppliers and dilutions are provided in Table S1.

Human and mouse sections were boiled in antigen unmasking solution (Vector Labs) and pre-incubated at room temperature for 1 h in blocking solution containing 10% normal donkey serum (Millipore), 1% bovine serum albumin (Sigma) and 0.2% Triton X-100 (Sigma). Sections were incubated with primary antibodies diluted in blocking solution at 4°C overnight followed by washing with blocking solution (3×15 min). Sections were then incubated with fluorophore-conjugated secondary antibodies (Invitrogen; diluted 1:1000 in blocking solution) for 1 h at room temperature, washed (3×15 min), counterstained with Hoechst nuclear stain (10 min at room temperature) and mounted (Fluoromount, SouthernBiotech).

The Operetta high-content microscope (PerkinElmer) was used for automated image acquisition of cell cultures. Images were then quantified using automated quantification pipelines developed using Columbus Image Analysis Software (PerkinElmer).

Tissue sections (both embryonic and P15) were imaged on an SP8 confocal microscope (Leica) and quantified manually using Fiji CellCounter plug-in. For quantification of embryonic tissue, adjacent sections were used for labelling (FoxA2, Ki67, Nurr1 and TH) and five sections spanning the anterior–posterior axis were counted per stain and sample. For P15 brain, TH^+ mDA neurons were quantified in sections at three rostrocaudal levels (Bregma: −2.92, −3.40 and −3.88 mm). TH^+, TH^+ $Girk2^+$ and TH^+ $calbindin^+$ cells were counted bilaterally for each level. Tissue sections were quantified while blinded to genotype.

RNAscope

RNAscope mRNA detection was performed according to the manual, using the RNAScope 2.5 HD reagent Kit-RED (ACD, 322350). PFA-fixed sections (10 µm) were dehydrated in an ethanol gradient (50%, 70% and 100%) and incubated with H_2O_2 for 10 min. Sections were washed in deionised water, boiled for 5 min in antigen retrieval solution and then transferred to a dish containing distilled water. After washing, slides were rinsed in fresh 100% ethanol and air dried. RNAscope Protease Plus was applied to the slides and incubated for 30 min at 40°C. Slides were then washed in distilled water with slight agitation. The appropriate RNAscope probe (Shh, catalogue no. 314361; Wnt1, catalogue no. 401091) was then applied to the slide and incubated for 2 h at 40°C. Sections were then washed in wash buffer and the colour reaction performed according to the user manual. Sections were counterstained for 1 min with haematoxylin (Scientific Laboratories, GHS132-1L) and the blue reaction performed using 0.02% ammonia water. Sections were dried at 60°C and mounted.

Acknowledgements

The authors acknowledge Drs Eoghan O'Duibhir and Bertrand Vernay for assistance with imaging and image quantification software. The human embryonic and fetal material was provided by the Joint MRC/Wellcome Trust (MR/R006237/1) Human Developmental Biology Resource (www.hdbr.org).

Competing interests

The authors declare no competing or financial interests.

Author contributions

Conceptualization: M.A., E.A., M.L.F., C.f.-C.; Methodology: M.A., L.N.M.; Validation: M.A.; Formal analysis: M.A.; Investigation: M.A.; Resources: L.N.M., M.L.F.; Writing - original draft: M.A., C.f.-C.; Writing - review & editing: L.N.M., E.A., M.L.F., C.f.-C.; Visualization: M.A.; Supervision: E.A., M.L.F., C.f.-C.; Project administration: M.A., C.f.-C.; Funding acquisition: E.A., C.f.-C.

Funding

C.f.-C. is supported by a European Union FP7 Neurostemcellrepair grant (602278), a National Institutes of Health grant (5R01EB016629-04) and a Wellcome Trust Senior Investigator Award. E.A. is supported by the Vetenskapsrådet (VR 2016-01526), the Stiftelsen för strategisk forskning (SB16-0065), the European Commission (NeuroStemCellRepair), Hjärnfonden (FO2017:0059), Cancerfonden (CAN 2016/572) and SFO Strat Regen at the Karolinska Institutet (SG-2018). Deposited in PMC for release after 6 months.

Supplementary information

Supplementary information available online at
http://dev.biologists.org/lookup/doi/10.1242/dev.172668.supplemental

References

Ahmed, M. and ffrench-Constant, C. (2016). Extracellular matrix regulation of stem cell behavior. *Curr Stem Cell Rep.* **2**, 197-206. doi:10.1007/s40778-016-0056-2

Alexander, G. E. (2004). Biology of Parkinson's disease: pathogenesis and pathophysiology of a multisystem neurodegenerative disorder. *Dialogues Clin. Neurosci.* **6**, 259-280.

Anderson, C., Winder, S. J. and Borycki, A.-G. (2007). Dystroglycan protein distribution coincides with basement membranes and muscle differentiation during mouse embryogenesis. *Dev. Dyn. Off. Publ. Am. Assoc. Anat.* **236**, 2627-2635. doi:10.1002/dvdy.21259

Bayer, S. A., Wills, K. V., Triarhou, L. C. and Ghetti, B. (1995). Time of neuron origin and gradients of neurogenesis in midbrain dopaminergic neurons in the mouse. *Exp. Brain Res.* **105**, 191-199. doi:10.1007/BF00240955

Bedford, L., Walker, R., Kondo, T., Van Cruchten, I., King, E. R. and Sablitzky, F. (2005). Id4 is required for the correct timing of neural differentiation. *Dev. Biol.* **280**, 386-395. doi:10.1016/j.ydbio.2005.02.001

Berti, C., Bartesaghi, L., Ghidinelli, M., Zambroni, D., Figlia, G., Chen, Z.-L., Quattrini, A., Wrabetz, L. and Feltri, M. L. (2011). Non-redundant function of dystroglycan and beta1 integrins in radial sorting of axons. *Dev. Camb. Engl.* **138**, 4025-4037. doi:10.1242/dev.065490

Bertini, E., D'amico, A., Gualandi, F. and Petrini, S. (2011). Congenital muscular dystrophies: a brief review. *Semin. Pediatr. Neurol.* **18**, 277-288. doi:10.1016/j.spen.2011.10.010

Blaess, S., Graus-Porta, D., Belvindrah, R., Radakovits, R., Pons, S. and Littlewood-Evans, A. (2004). Beta1-integrins are critical for cerebellar granule cell precursor proliferation. *J. Neurosci. Off. J. Soc. Neurosci.* **24**, 3402-3412. doi:10.1523/JNEUROSCI.5241-03.2004

Blum, K., Chen, A. L.-C., Braverman, E. R., Comings, D. E., Chen, T. J., Arcuri, V., Blum, S. H., Downs, B. W., Waite, R. L. and Notaro, A. (2008). Attention-deficit-hyperactivity disorder and reward deficiency syndrome. *Neuropsychiatr. Dis. Treat.* **4**, 893-918. doi:10.2147/NDT.S2627

Britto, J., Tannahill, D. and Keynes, R. (2002). A critical role for sonic hedgehog signaling in the early expansion of the developing brain. *Nat. Neurosci.* **5**, 103-110. doi:10.1038/nn797

Bye, C. R., Thompson, L. H. and Parish, C. L. (2012). Birth dating of midbrain dopamine neurons identifies A9 enriched tissue for transplantation into parkinsonian mice. *Exp. Neurol.* **236**, 58-68. doi:10.1016/j.expneurol.2012.04.002

Chan, J. A., Balasubramanian, S., Witt, R. M., Nazemi, K. J., Choi, Y., Pazyra-Murphy, M. F., Walsh, C. O., Thompson, M. and Segal, R. A. (2009). Proteoglycan interactions with Sonic Hedgehog specify mitogenic responses. *Nat. Neurosci.* **12**, 409-417. doi:10.1038/nn.2287

Clement, E., Mercuri, E., Godfrey, C., Smith, J., Robb, S., Kinali, M., Straub, V., Bushby, K., Manzur, A., Talim, B. et al. (2008). Brain involvement in muscular dystrophies with defective dystroglycan glycosylation. *Ann. Neurol.* **64**, 573-582. doi:10.1002/ana.21482

Fietz, S. A., Lachmann, R., Brandl, H., Kircher, M., Samusik, N., Schroder, R., Lakshmanaperumal, N., Henry, I., Vogt, J., Riehn, A. et al. (2012). Transcriptomes of germinal zones of human and mouse fetal neocortex suggest a role of extracellular matrix in progenitor self-renewal. *Proc. Natl. Acad. Sci. USA* **109**, 11836-11841. doi:10.1073/pnas.1209647109

Grace, A. A. (2016). Dysregulation of the dopamine system in the pathophysiology of schizophrenia and depression. *Nat. Rev. Neurosci.* **17**, 524-532. doi:10.1038/nrn.2016.57

Haas, T. L., Sciuto, M. R., Brunetto, L., Valvo, C., Signore, M., Fiori, M. E., di Martino, S., Giannetti, S., Morgante, L., Boe, A. et al. (2017). Integrin alpha7 is a functional marker and potential therapeutic target in glioblastoma. *Cell Stem Cell* **21**, 35-50.e9. doi:10.1016/j.stem.2017.04.009

Hatakeyama, J., Bessho, Y., Katoh, K., Ookawara, S., Fujioka, M. and Guillemot, F. (2004). Hes genes regulate size, shape and histogenesis of the nervous system by control of the timing of neural stem cell differentiation. *Dev. Camb. Engl.* **131**, 5539-5550. doi:10.1242/dev.01436

Helbling-Leclerc, A., Zhang, X., Topaloglu, H., Cruaud, C., Tesson, F., Weissenbach, J., Tomé, F. M. S., Schwartz, K., Fardeau, M., Tryggvason, K. et al. (1995). Mutations in the laminin alpha 2-chain gene (LAMA2) cause merosin-deficient congenital muscular dystrophy. *Nat. Genet.* **11**, 216-218. doi:10.1038/ng1095-216

Ishibashi, M. and Mcmahon, A. P. (2002). A sonic hedgehog-dependent signaling relay regulates growth of diencephalic and mesencephalic primordia in the early mouse embryo. *Dev. Camb. Engl.* **129**, 4807-4819.

Jiang, F. X., Georges-Labouesse, E. and Harrison, L. C. (2001). Regulation of laminin 1-induced pancreatic beta-cell differentiation by alpha6 integrin and alpha-dystroglycan. *Mol. Med. Camb. Mass.* **7**, 107-114. doi:10.1007/BF03401944

Jones, K. J., Morgan, G., Johnston, H., Tobias, V., Ouvrier, R. A., Wilkinson, I. and North, K. N. (2001). The expanding phenotype of laminin alpha2 chain (merosin) abnormalities: case series and review. *J. Med. Genet.* **38**, 649-657. doi:10.1136/jmg.38.10.649

Kabanova, A., Pabst, M., Lorkowski, M., Braganza, O., Boehlen, A., Nikbakht, N., Pothmann, L., Vaswani, A. R., Musgrove, R., Di Monte, D. A. et al. (2015). Function and developmental origin of a mesocortical inhibitory circuit. *Nat. Neurosci.* **18**, 872-882. doi:10.1038/nn.4020

Kazanis, I., Lathia, J. D., Vadakkan, T. J., Raborn, E., Wan, R., Mughal, M. R., Eckley, D. M., Sasaki, T., Patton, B., Mattson, M. P. et al. (2010). Quiescence and activation of stem and precursor cell populations in the subependymal zone of the mammalian brain are associated with distinct cellular and extracellular matrix signals. *J. Neurosci. Off. J. Soc. Neurosci.* **30**, 9771-9781. doi:10.1523/JNEUROSCI.0700-10.2010

Kele, J., Simplicio, N., Ferri, A. L. M., Mira, H., Guillemot, F., Arenas, E. and Ang, S. L. (2006). Neurogenin 2 is required for the development of ventral midbrain dopaminergic neurons. *Dev. Camb. Engl.* **133**, 495-505. doi:10.1242/dev.02223

Kirkeby, A., Nelander, J. and Parmar, M. (2012). Generating regionalized neuronal cells from pluripotency, a step-by-step protocol. *Front. Cell Neurosci.* **6**, 64. doi:10.3389/fncel.2012.00064

Lai, T., Jabaudon, D., Molyneaux, B. J., Azim, E., Arlotta, P., Menezes, J. R. L. and Macklis, J. D. (2008). SOX5 controls the sequential generation of distinct corticofugal neuron subtypes. *Neuron* **57**, 232-247. doi:10.1016/j.neuron.2007.12.023

La Manno, G., Gyllborg, D., Codeluppi, S., Nishimura, K., Salto, C., Zeisel, A., Borm, L. E., Stott, S. R. W., Toledo, E. M., Villaescusa, J. C. et al. (2016). Molecular diversity of midbrain development in mouse, human, and stem cells. *Cell* **167**, 566-580.e19. doi:10.1016/j.cell.2016.09.027

Lathia, J. D., Patton, B., Eckley, D. M., Magnus, T., Mughal, M. R., Sasaki, T., Caldwell, M. A., Rao, M. S., Mattson, M. P. and ffrench-Constant, C. (2007). Patterns of laminins and integrins in the embryonic ventricular zone of the CNS. *J. Comp. Neurol.* **505**, 630-643. doi:10.1002/cne.21520

Lathia, J. D., Gallagher, J., Heddleston, J. M., Wang, J., Eyler, C. E., Macswords, J., Wu, Q., Vasanji, A., McLendon, R. E., Hjelmeland, A. B. et al. (2010). Integrin alpha 6 regulates glioblastoma stem cells. *Cell Stem Cell* **6**, 421-432. doi:10.1016/j.stem.2010.02.018

Lathia, J. D., Li, M., Hall, P. E., Gallagher, J., Hale, J. S., Wu, Q., Venere, M., Levy, E., Rani, M. R. S., Huang, P. et al. (2012). Laminin alpha 2 enables glioblastoma stem cell growth. *Ann. Neurol.* **72**, 766-778. doi:10.1002/ana.23674

Long, K., Moss, L., Laursen, L., Boulter, L. and ffrench-Constant, C. (2016). Integrin signalling regulates the expansion of neuroepithelial progenitors and neurogenesis via Wnt7a and Decorin. *Nat. Commun.* **7**, 10354. doi:10.1038/ncomms10354

Loulier, K., Lathia, J. D., Marthiens, V., Relucio, J., Mughal, M. R., Tang, S.-C., Coksaygan, T., Hall, P. E., Chigurupati, S., Patton, B. et al. (2009). beta1 integrin maintains integrity of the embryonic neocortical stem cell niche. *PLoS Biol.* **7**, e1000176. doi:10.1371/journal.pbio.1000176

Mercuri, E., Gruter-Andrew, J., Philpot, J., Sewry, C., Counsell, S., Henderson, S., Jensen, A., Naom, I., Bydder, G., Dubowitz, V. et al. (1999). Cognitive abilities in children with congenital muscular dystrophy: correlation with brain MRI and merosin status. *Neuromuscul Disord NMD* **9**, 383-387. doi:10.1016/S0960-8966(99)00034-6

Miyagoe, Y., Hanaoka, K., Nonaka, I., Hayasaka, M., Nabeshima, Y., Arahata, K., Nabeshima, Y.-i and Takeda, S. (1997). Laminin alpha2 chain-null mutant mice by targeted disruption of the Lama2 gene: a new model of merosin (laminin 2)-deficient congenital muscular dystrophy. *FEBS Lett.* **415**, 33-39. doi:10.1016/S0014-5793(97)01007-7

Morales, M. and Margolis, E. B. (2017). Ventral tegmental area: cellular heterogeneity, connectivity and behaviour. *Nat. Rev. Neurosci.* **18**, 73-85. doi:10.1038/nrn.2016.165

Morgner, J., Ghatak, S., Jakobi, T., Dieterich, C., Aumailley, M. and Wickstrom, S. A. (2015). Integrin-linked kinase regulates the niche of quiescent epidermal stem cells. *Nat. Commun.* **6**, 8198. doi:10.1038/ncomms9198

Nascimento, M. A., Sorokin, L. and Coelho-Sampaio, T. (2018). Fractone bulbs derive from ependymal cells and their laminin composition influence the stem cell niche in the subventricular zone. *J. Neurosci. Off. J. Soc. Neurosci.* **38**, 3880-3889. doi:10.1523/JNEUROSCI.3064-17.2018

Nishiuchi, R., Murayama, O., Fujiwara, H., Gu, J., Kawakami, T., Aimoto, S., Wada, Y. and Sekiguchi, K. (2003). Characterization of the ligand-binding specificities of integrin alpha3beta1 and alpha6beta1 using a panel of purified laminin isoforms containing distinct alpha chains. *J. Biochem. (Tokyo)* **134**, 497-504. doi:10.1093/jb/mvg185

Nutt, D. J., Lingford-Hughes, A., Erritzoe, D. and Stokes, P. R. A. (2015). The dopamine theory of addiction: 40 years of highs and lows. *Nat. Rev. Neurosci.* **16**, 305-312. doi:10.1038/nrn3939

Philpot, J., Cowan, F., Pennock, J., Sewry, C., Dubowitz, V., Bydder, G. and Muntoni, F. (1999). Merosin-deficient congenital muscular dystrophy: the spectrum of brain involvement on magnetic resonance imaging. *Neuromuscul Disord NMD* **9**, 81-85. doi:10.1016/S0960-8966(98)00110-2

Poitelon, Y., Lopez-Anido, C., Catignas, K., Berti, C., Palmisano, M., Williamson, C., Ameroso, D., Abiko, K., Hwang, Y., Gregorieff, A. et al. (2016). YAP and TAZ control peripheral myelination and the expression of laminin receptors in Schwann cells. *Nat. Neurosci.* **19**, 879-887. doi:10.1038/nn.4316

Pollen, A. A., Nowakowski, T. J., Chen, J., Retallack, H., Sandoval-Espinosa, C., Nicholas, C. R., Shuga, J., Liu, S. J., Oldham, M. C., Diaz, A. et al. (2015). Molecular identity of human outer radial glia during cortical development. *Cell* **163**, 55-67. doi:10.1016/j.cell.2015.09.004

Ricotti, V., Mandy, W. P. L., Scoto, M., Pane, M., Deconinck, N., Messina, S., Mercuri, E., Skuse, D. H. and Muntoni, F. (2016). Neurodevelopmental, emotional, and behavioural problems in Duchenne muscular dystrophy in relation to underlying dystrophin gene mutations. *Dev. Med. Child Neurol.* **58**, 77-84. doi:10.1111/dmcn.12922

Rozario, T. and Desimone, D. W. (2010). The extracellular matrix in development and morphogenesis: a dynamic view. *Dev. Biol.* **341**, 126-140. doi:10.1016/j.ydbio.2009.10.026

Schofield, J. N., Gorecki, D. C., Blake, D. J., Davies, K. and Edwards, Y. H. (1995). Dystroglycan mRNA expression during normal and mdx mouse embryogenesis: a comparison with utrophin and the apo-dystrophins. *Dev. Dyn. Off. Publ. Am. Assoc. Anat.* **204**, 178-185. doi:10.1002/aja.1002040208

Sframeli, M., Sarkozy, A., Bertoli, M., Astrea, G., Hudson, J., Scoto, M., Mein, R., Yau, M., Phadke, R., Feng, L. et al. (2017). Congenital muscular dystrophies in the UK population: clinical and molecular spectrum of a large cohort diagnosed over a 12-year period. *Neuromuscul Disord NMD* **27**, 793-803. doi:10.1016/j.nmd.2017.06.008

Shen, Q., Wang, Y., Kokovay, E., Lin, G., Chuang, S.-M., Goderie, S. K., Roysam, B. and Temple, S. (2008). Adult SVZ stem cells lie in a vascular niche: a quantitative analysis of niche cell-cell interactions. *Cell Stem Cell* **3**, 289-300. doi:10.1016/j.stem.2008.07.026

Suzuki, Y., Higuchi, S., Aida, I., Nakajima, T. and Nakada, T. (2017). Abnormal distribution of GABAA receptors in brain of duchenne muscular dystrophy patients. *Muscle Nerve.* **55**, 591-595. doi:10.1002/mus.25383

Talts, J. F., Andac, Z., Gohring, W., Brancaccio, A. and Timpl, R. (1999). Binding of the G domains of laminin alpha1 and alpha2 chains and perlecan to heparin, sulfatides, alpha-dystroglycan and several extracellular matrix proteins. *EMBO J.* **18**, 863-870. doi:10.1093/emboj/18.4.863

Tan, X., Liu, W. A., Zhang, X.-J., Shi, W., Ren, S.-Q., Li, Z., Brown, K. N. and Shi, S.-H. (2016). Vascular influence on ventral telencephalic progenitors and neocortical interneuron production. *Dev. Cell* **36**, 624-638. doi:10.1016/j.devcel.2016.02.023

Wright, K. M., Lyon, K. A., Leung, H., Leahy, D. J., Ma, L. and Ginty, D. D. (2012). Dystroglycan organizes axon guidance cue localization and axonal pathfinding. *Neuron* **76**, 931-944. doi:10.1016/j.neuron.2012.10.009

Yurchenco, P. D., Mckee, K. K., Reinhard, J. R. and Ruegg, M. A. (2017). Laminin-deficient muscular dystrophy: molecular pathogenesis and structural repair strategies. *Matrix Biol.* 71-72, 174-187. doi:10.1016/j.matbio.2017.11.009

Zhang, D., Yang, S., Toledo, E. M., Gyllborg, D., Saltó, C., Carlos Villaescusa, J. and Arenas, E. (2017). Niche-derived laminin-511 promotes midbrain dopaminergic neuron survival and differentiation through YAP. *Sci. Signal.* **10**. doi:10.1126/scisignal.aal4165

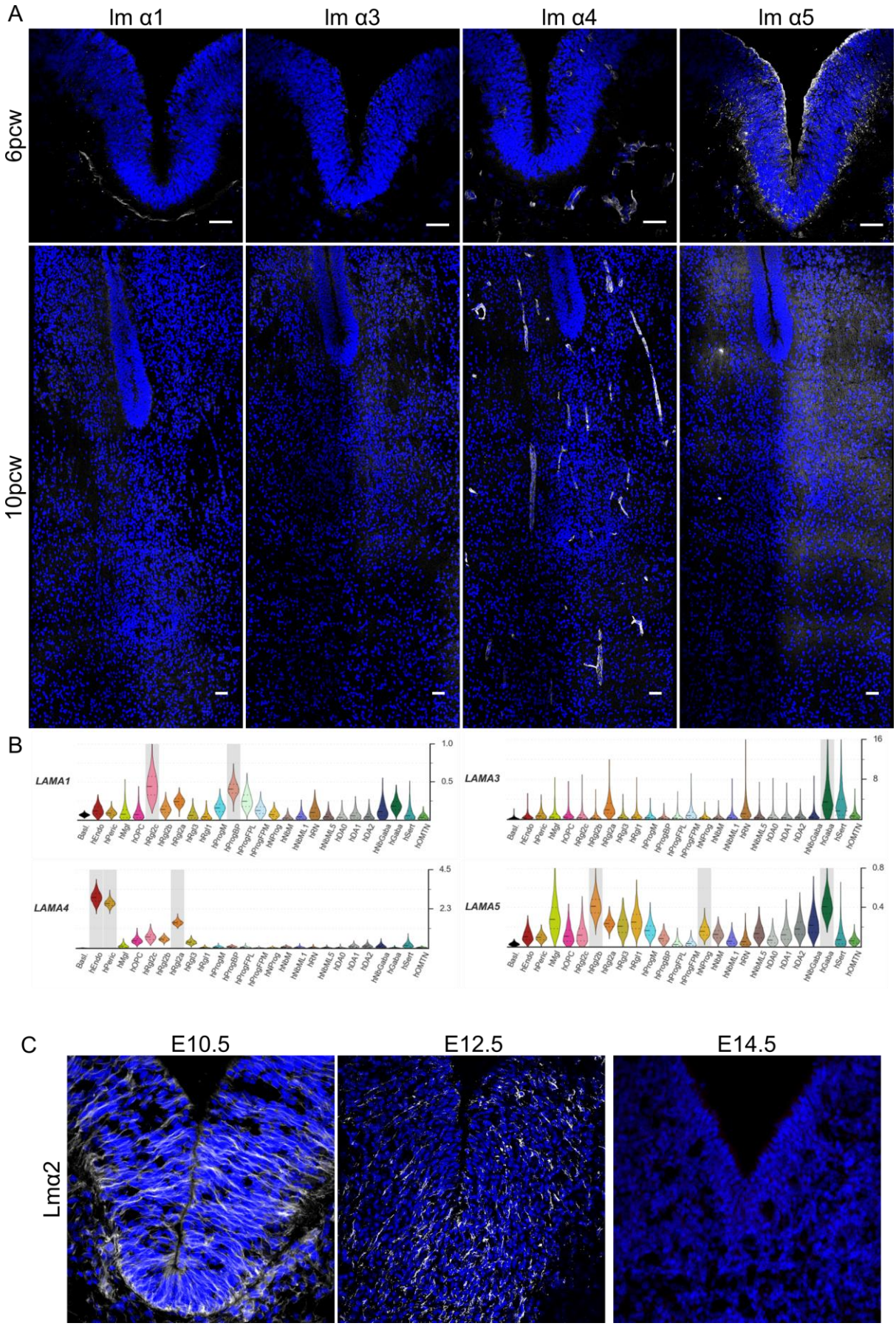

Fig S1: Lm-α chain immunohistochemistry in human VM
(A) Lm-α1 expression is restricted to the basement membrane surrounding the basal surface neural tube. Lm-a3 is not expressed in the human VM. Lm-a4 is restricted to the basal laminae of blood vessels at both 6 and 10 pcw. Meanwhile lm-a5 is expressed on both the ventricular and basal surfaces of the VM at 6 pcw as well as some interstitial expression. (B) scRNA-seq data of individual lm-a chains showing cell types for gene expression in human development. Right axis shows absolute molecule counts. (C) Lm-α2 expression in the mouse VM at E10.5-E14.5 displays a similar expression pattern as that seen in the human embryo. Expression can be seen to diminish over time with negligible positive expression at E14.5.

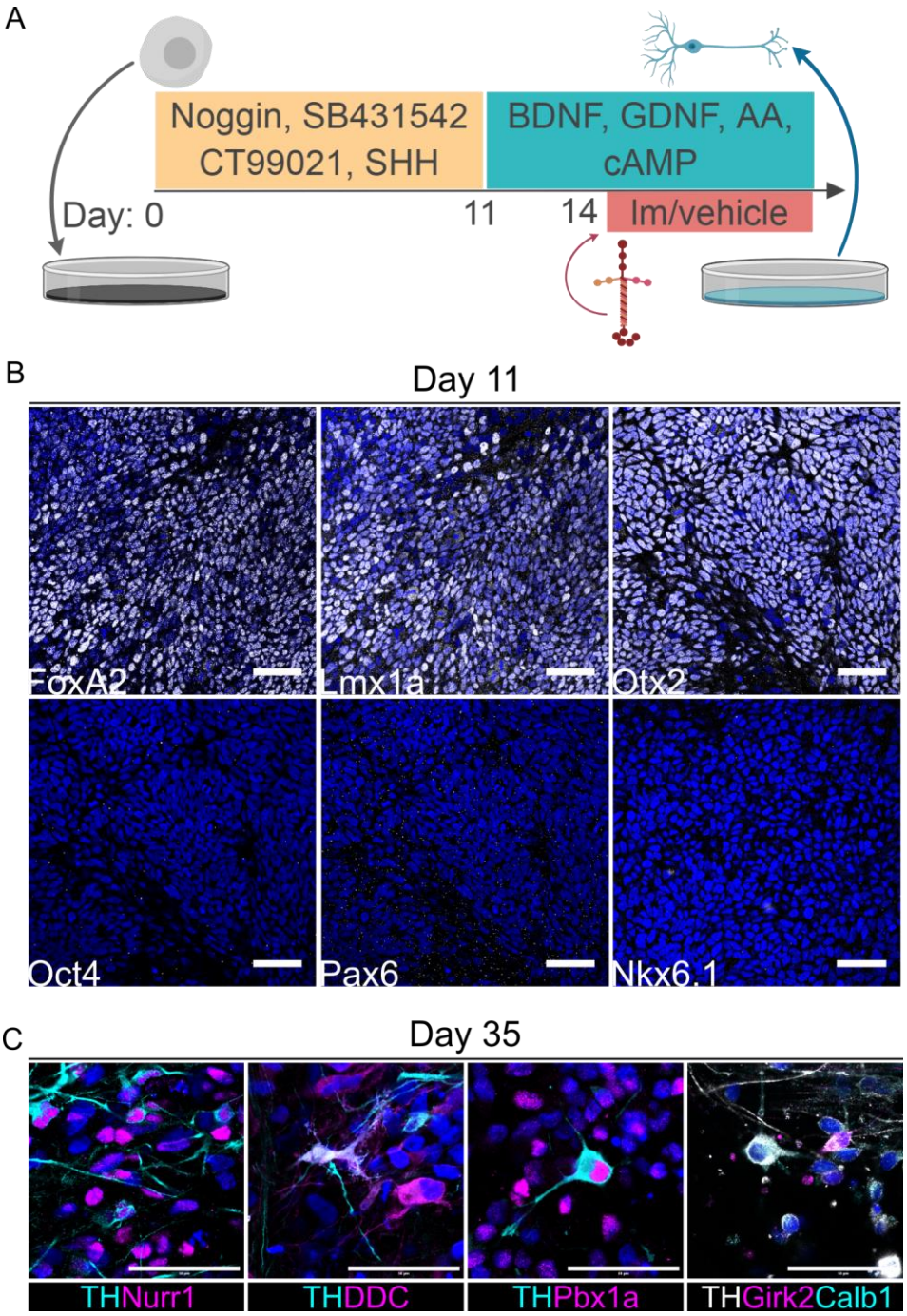

Fig S2: Differentiation protocol and patterning of hES cells into mDA progenitors
(A) schematic of hES differentiation protocol with Im treatment at day 14 till fixation. (B) Immunostainings of day 11 cultures showing cultures to be triple positive for the mDA progenitor markers FoxA2, Lmx1a and Otx2. Cultures are negative for the pluripotency marker Oct4, forebrain marker Pax6 and the lateral domain marker Nkx6.1. (C) TH+ Neurons at day 35 showing positive immunoreactivity for a panel of markers (Nurr1, Pbx1a, DDC, Calb1, Girk2) illustrative of bona fide mDA neurons. Scale bar 50µm.

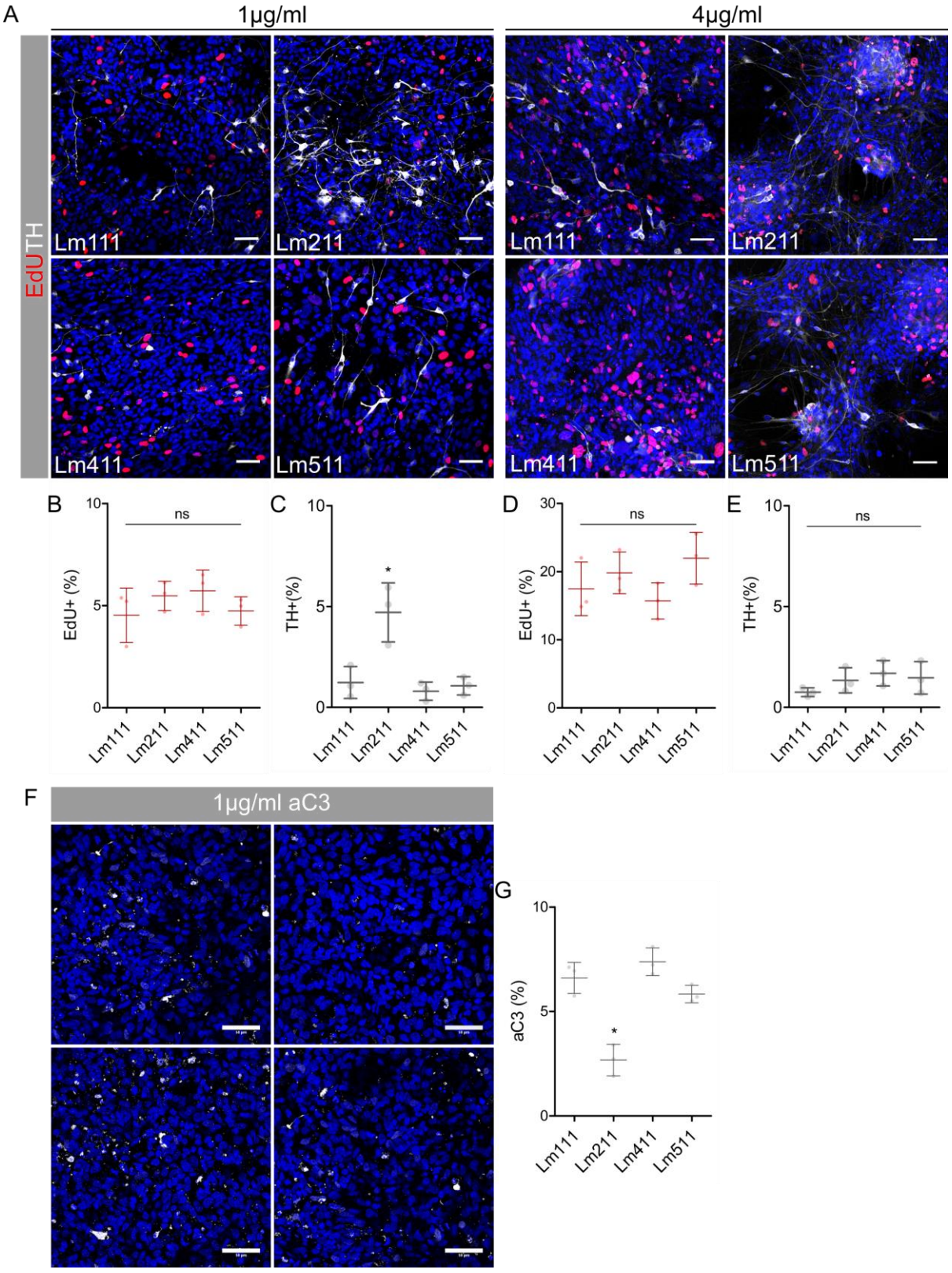

Fig S3: Lm isoform specificity in regulating mDA progenitor proliferation and survival
(A) Representative images of mDA cultures at day 28 exposed to lm211 at 1 and 4 µgml^{-1}, staining for proliferation (EdU) and neurons (TH). At low concentrations (1 µgml^{-1}), no significant difference in proliferation (B) is detected between any of the lm isoforms whilst an increase in TH+ mDA neurons (C) is observed on lm211. At high concentrations (4 µgml^{-1}), no differences are detected in the number of mDA progenitors that are EdU+ (D) or TH+ (E). (F,G) Significantly fewer aC3^{+} cells can be seen at 1 µgml-1 of lm211 suggesting the increase in TH^{+} neurons is due to increased survival.
*p<0.001, ANOVA Tukeys post test, N=3

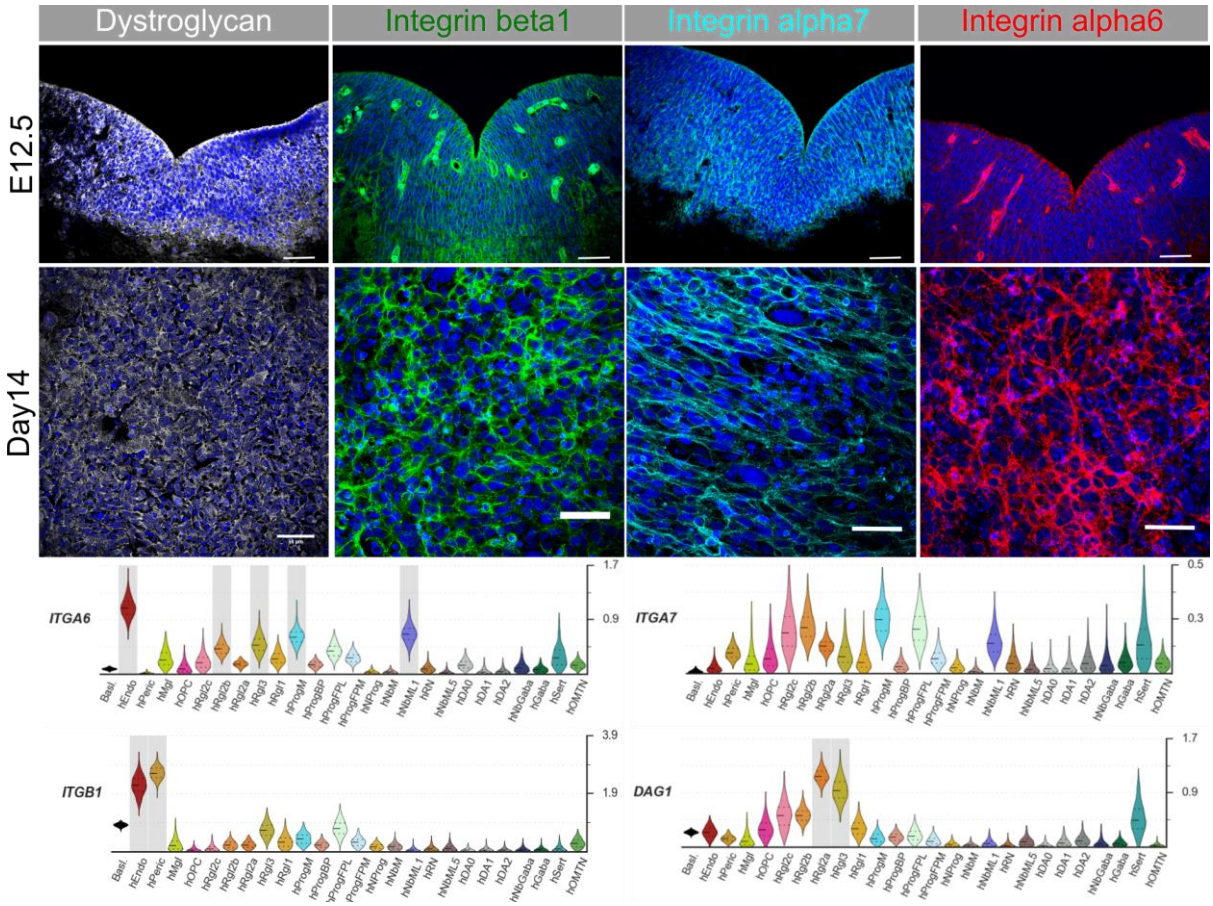

Fig S4: Expression of lm receptors
Integrins α6, α7, β1 and Dystroglycan are expressed in the mouse VM and on hES derived mDA progenitors at day 14 of culture. scRNA-seq of the hVM identifies radial glial (hRgl1-3) and VM progenitors (hProg) positive for lm receptor expression. Right axis shows absolute molecule counts. Scale bar 50μm.

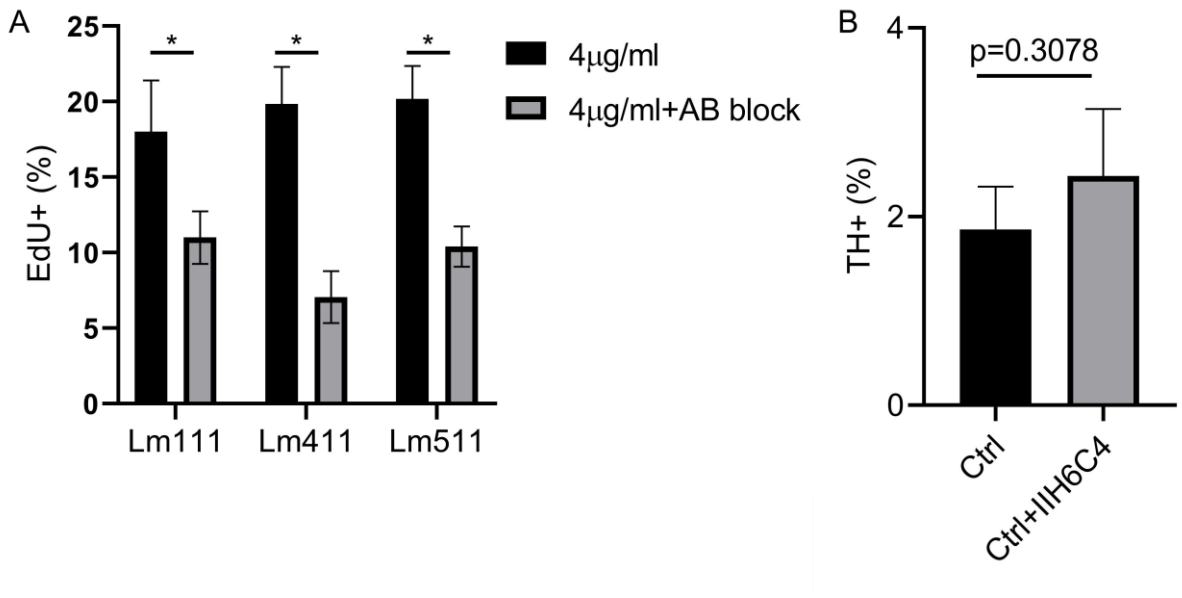

Fig S5: Specificity of laminin-receptor interactions
(A) Integrin α6 and α7 blocked with antibodies in the presence of 4 μgml^{-1} of lm111, lm411 and lm511. When cultures are exposed to the integrin blocking antibodies, the lm-driven increase in proliferation is abrogated suggesting that the integrin receptors are mediating the proliferative effects of lm. (B) Blocking the α-dystroglycan receptor with no exogenous lm211 does not effect the number of TH+ neurons generated. N=3, two-tailed unpaired t-test, *p<0.001.

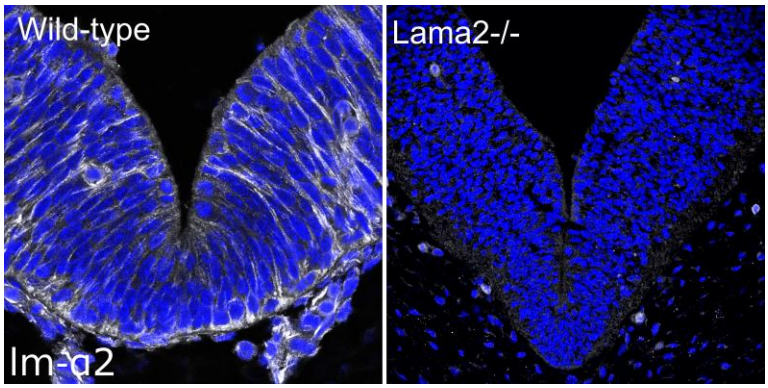

Fig S6: Lm-α2 expression in the wild-type and lama2$^{-/-}$ mouse VM
No Lm-α2 expression can be detected in the lama2$^{-/-}$ embryos confirming the knock-out.

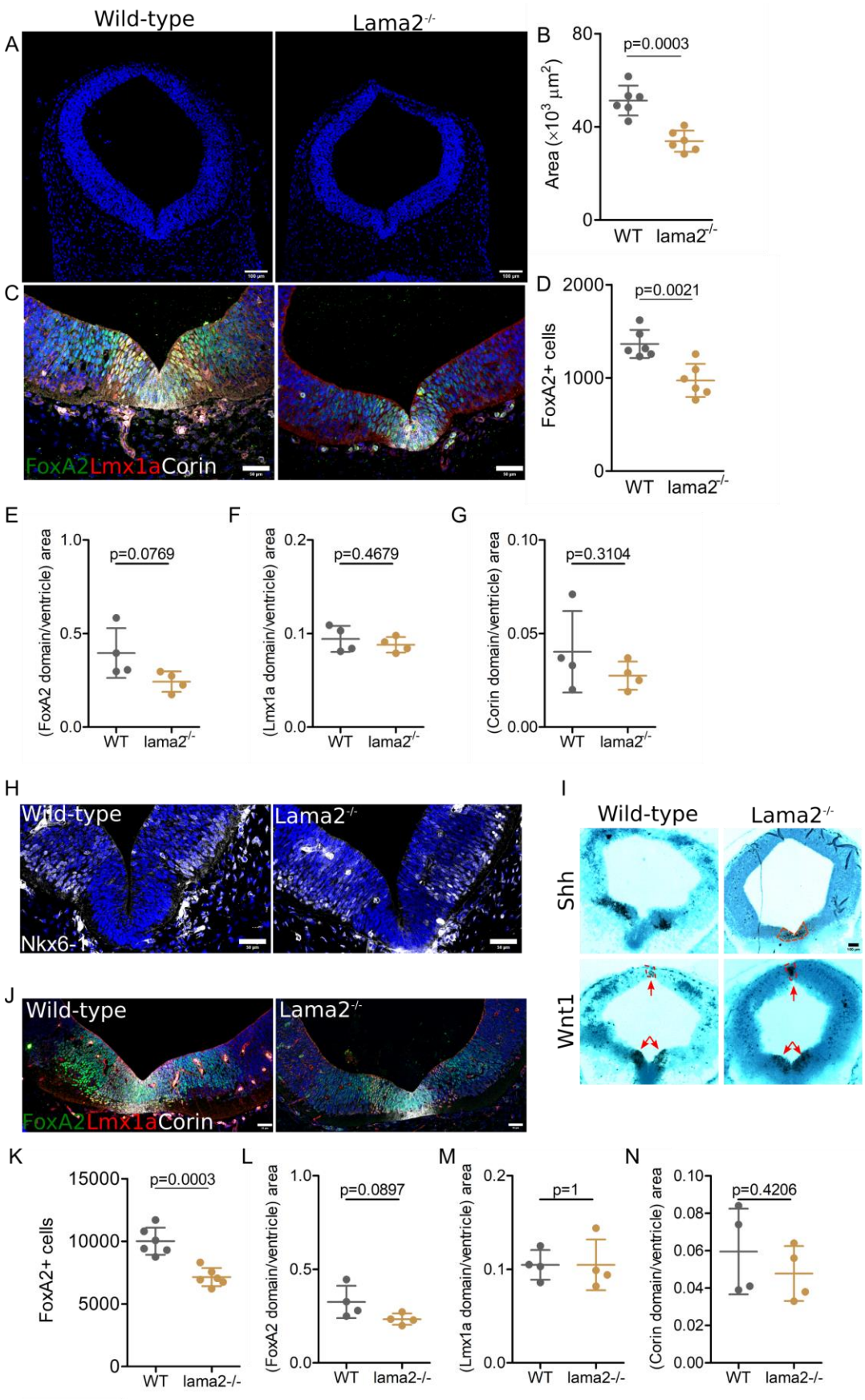

Fig S7: Lama2$^{-/-}$ exhibit defects in growth but normal patterning
(A) Cross-sections of wild-type and lama2$^{-/-}$ mesencephalon at E10.5 (scale bar 100 µm) with the mutant mesencephalon significantly smaller in area (B). The dopaminergic domain consisting of

FoxA2, Lmx1a and Corin (scale bar 50 μm). Fewer FoxA2 cells are present in the lama2$^{-/-}$ midbrain (D). The area of each domain was calculated and normalised to the area of the ventricle. No significant differences were detected in the size of the normalised FoxA2 (E), Lmx1a (F) and Corin (G). Nkx6-1+ cells can be seen laterally and are induced in both the mutant and wild-type embryo at E10.5 (scale bar 50 μm) (H). Potential ectopic expression and a delay in the lateral expansion and medial inhibition of Shh expression in the mutant embryos at E12.5 can be seen. Wnt1 expression is comparable to wild-type and previously published reports (scale bar 100 μm) (I). Dopaminergic domain remains smaller at E12.5 (scale bar 50 μm) (J) in the mutant embryo compared to wild-type, consisting of fewer FoxA2 cells (K) but when normalised for ventricle size, there are no significant differences in FoxA2 (L), Lmx1a (M) or Corin (N) domain size. N=4-6, two-tailed unpaired t-test.

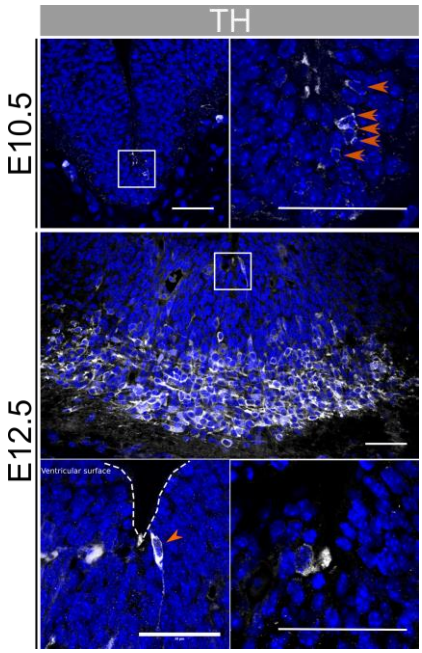

Fig S8: Ectopic mDA neurons in the VM of lama2$^{-/-}$ embryos
TH+ mDA neurons can be seen lining the ventricular surface of lm-α2 null embryos at E10.5 (orange arrows). Ectopic mDA neurons (orange arrowhead) at the ventricular surface (dashed line) continue to be observed at E12.5. Scale bar 50 μm.

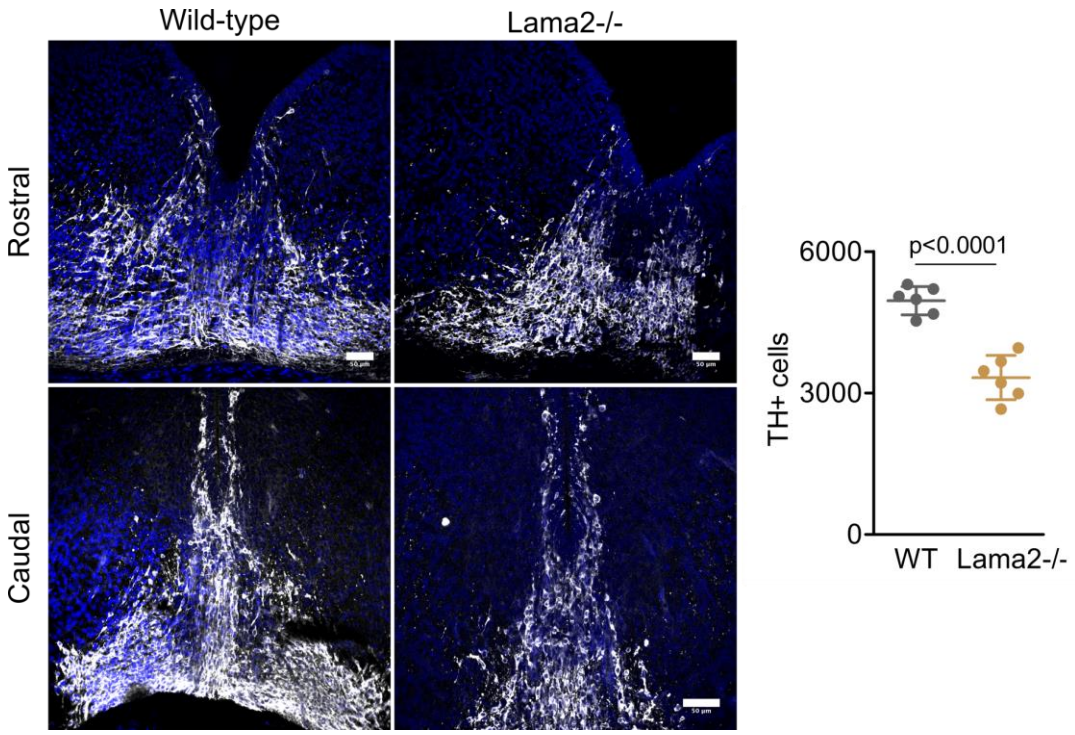

Fig S9: Reduced mDA neurons in the VM at E14.5
Significantly fewer TH+ mDA neurons in the VM of mutant embryos compared to wild-type littermate controls. N=6, two-tailed unpaired t-test, scale bar 50 µm.

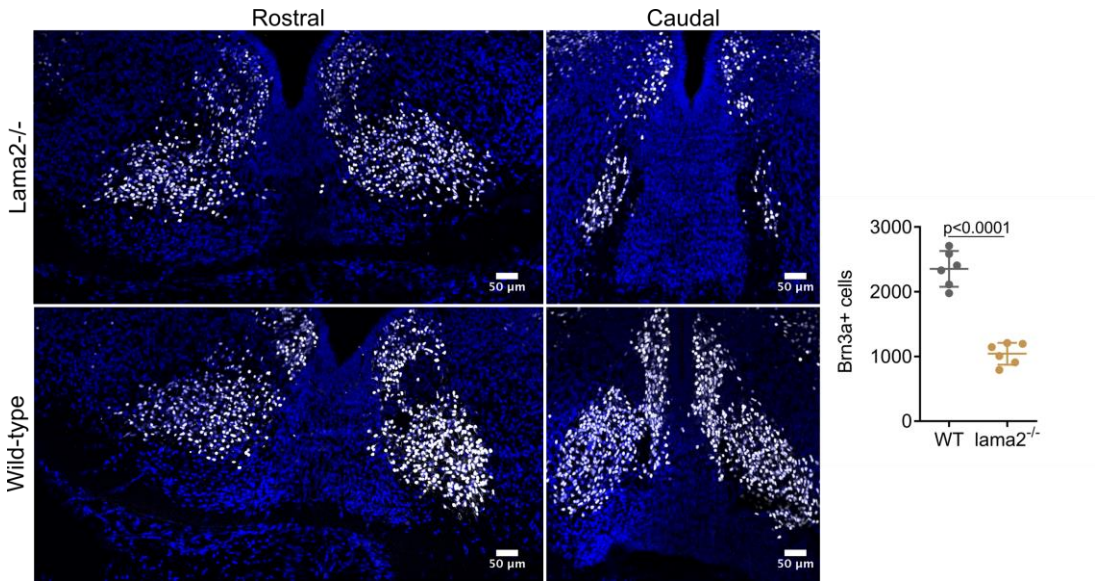

Fig S10: Development of non-mDA VM neurons compromised in lama2$^{-/-}$ mutants.
Brn3a+ red nucleus neurons, derived from FoxA2+ progenitors, are significantly reduced in the mutant embryos compared to wild-type littermate controls at E14.5. N=6, two-tailed unpaired t-test, scale bar 50µm.

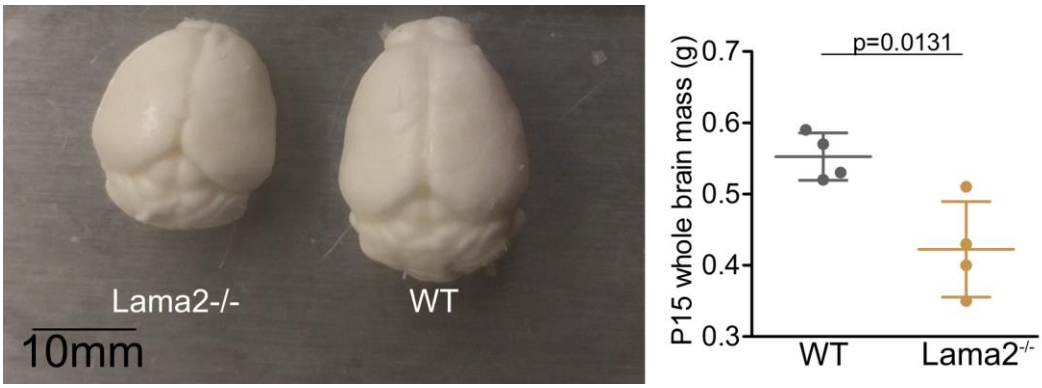

Fig S11: Smaller mutant brains compared to wild-types at P15
Lama2$^{-/-}$ brains are significantly smaller than WT littermate controls, quantified via mass. N=4, two-tailed unpaired t-test.

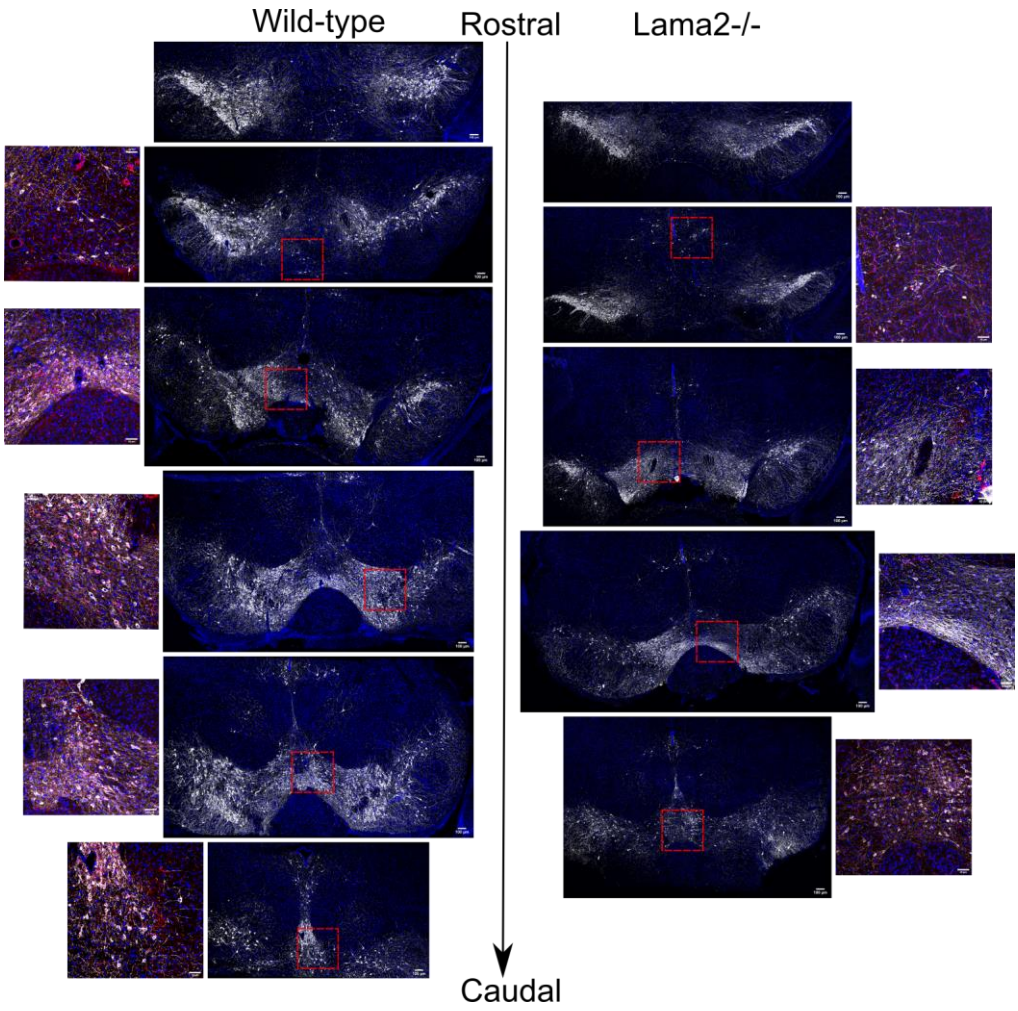

Fig S12: VM of wild-type and mutant P15 brains showing reduced number of neurons
Large panels are images of the whole VM from wild-type and lama2$^{-/-}$ P15 brains along the rostral-caudal axis showing reduced TH+ immunoreactivity (white) in the mutant brains (scale bar 100 μm). Images to the side are expanded view of the red boxes displaying TH (white) and Calb1 (red) (scale bar 50 μm). Fewer TH+ Calb1+ double positive cells can be seen in the mutant brains, particularly in the more caudal sections.

Table S1: List of Antibodies and dilutions used in this study. References detailing specificity of antibodies are provided.

Protein	Species	Company (cat.no.)	Dilution	Reference
Laminin α1	Rabbit	Assay Biotech (C13064)	1:200	(Olsen et al., 1989)
Laminin α2	Rabbit	Assay Biotech (C13065)	1:200	(Yap et al., 2019)
Laminin α3	Rabbit	Assay Biotech (C13066)	1:200	(Ishihara et al., 2018)
Laminin α4	Goat	R&D (AF3837)	1:400	(Yao et al., 2014)
Laminin α5	Rabbit	Assay Biotech (C13068)	1:200	(Blanco et al., 2016)
Integrin α6 [GoH3]	Rat	R&D (MAB13501)	1:500	(Sonnenberg et al., 1987)
Integrin α7	Rabbit	Abcam (ab75224)	1:500	(Previtali et al., 2003)
Integrin β1 [MB1.2]	Rat	Millipore (MAB1997)	1:500	(Von Ballestrem et al., 1996)
Dystroglycan [IIH6]	Mouse	SantaCruz (sc-53987)	1:1000	(Gee et al., 1994)
FoxA2 [M-20]	Goat	SantaCruz (sc-6554)	1:500	(Hatzis and Talianidis, 2002)
Ki67 [SP6]	Rabbit	Abcam (ab16667)	1:500	(Ekholm et al., 2014)
Nurr1 [N1404]	Mouse	Abcam (ab41917)	1:500	(Abasi et al., 2012)
TH	Rabbit	Millipore (AB152)	1:1000	(Ryczko et al., 2016)
Girk2	Goat	Abcam (ab65096)	1:500	(Fernandez-Alacid et al., 2011)
Calbindin	Mouse	Swant (300)	1:1000	(Martin del Campo et al., 2014)
Otx2	Goat	R&D (AF1979)	1:1000	(Sakai et al., 2017)
Oct4 [C-10]	Mouse	SantaCruz (sc-5279)	1:1000	(Kristensen et al., 2010)
Lmx1α	Rabbit	Millipore (AB10533)	1:1000	(Laguna et al., 2015)
Nkx6.1	Mouse	DHSB (1:50)	1:100	(Pedersen et al., 2006)
aCaspase 3 [ASP175]	Rabbit	Cell Signalling (9661s)	1:500	(Wang et al., 2017)
Pax6	Rabbit	Abcam (ab5790)	1:200	(Tan et al., 2016)
Ngn2 [C-16]	Goat	SantaCruz (sc-19233)	1:1000	(Mazzoni et al., 2013)
Corin [231443]	Rat	Invitrogen (231443)	1:500	(Paik et al., 2018)
DDC	Goat	R&D (AF3564-SP)	1:250	(Sandmeier et al., 1994)
Pbx1a [710.2]	Mouse	SantaCruz (sc-101851)	1:250	(Villaescusa et al., 2016)

Reference:

Abasi, M., Massumi, M., Riazi, G., Amini, H., 2012. The synergistic effect of beta-boswellic acid and Nurr1 overexpression on dopaminergic programming of antioxidant glutathione peroxidase-1-expressing murine embryonic stem cells. Neuroscience 222, 404–416. https://doi.org/10.1016/j.neuroscience.2012.07.009

Blanco, S., Bandiera, R., Popis, M., Hussain, S., Lombard, P., Aleksic, J., Sajini, A., Tanna, H., Cortes-Garrido, R., Gkatza, N., Dietmann, S., Frye, M., 2016. Stem cell function and stress response are controlled by protein synthesis. Nature 534, 335–340. https://doi.org/10.1038/nature18282

Ekholm, M., Beglerbegovic, S., Grabau, D., Lovgren, K., Malmstrom, P., Hartman, L., Ferno, M., 2014. Immunohistochemical assessment of Ki67 with antibodies SP6 and MIB1 in primary breast cancer: a comparison of prognostic value and reproducibility. Histopathology 65, 252–260. https://doi.org/10.1111/his.12392

Fernandez-Alacid, L., Watanabe, M., Molnar, E., Wickman, K., Lujan, R., 2011. Developmental regulation of G protein-gated inwardly-rectifying K+ (GIRK/Kir3) channel subunits in the brain. Eur. J. Neurosci. 34, 1724–1736. https://doi.org/10.1111/j.1460-9568.2011.07886.x

Gee, S.H., Montanaro, F., Lindenbaum, M.H., Carbonetto, S., 1994. Dystroglycan-alpha, a dystrophin-associated glycoprotein, is a functional agrin receptor. Cell 77, 675–686. https://doi.org/10.1016/0092-8674(94)90052-3

Hatzis, P., Talianidis, I., 2002. Dynamics of enhancer-promoter communication during differentiation-induced gene activation. Mol. Cell 10, 1467–1477.

Ishihara, J., Ishihara, A., Fukunaga, K., Sasaki, K., White, M.J.V., Briquez, P.S., Hubbell, J.A., 2018. Laminin heparin-binding peptides bind to several growth factors and enhance diabetic wound healing. Nat. Commun. 9, 2163. https://doi.org/10.1038/s41467-018-04525-w

Kristensen, D.M., Nielsen, J.E., Kalisz, M., Dalgaard, M.D., Audouze, K., Larsen, M.E., Jacobsen, G.K., Horn, T., Brunak, S., Skakkebaek, N.E., Leffers, H., 2010. OCT4 and downstream factors are expressed in human somatic urogenital epithelia and in culture of epididymal spheres. Mol. Hum. Reprod. 16, 835–845. https://doi.org/10.1093/molehr/gaq008

Laguna, A., Schintu, N., Nobre, A., Alvarsson, A., Volakakis, N., Jacobsen, J.K., Gomez-Galan, M., Sopova, E., Joodmardi, E., Yoshitake, T., Deng, Q., Kehr, J., Ericson, J., Svenningsson, P., Shupliakov, O., Perlmann, T., 2015. Dopaminergic control of autophagic-lysosomal function implicates Lmx1b in Parkinson's disease. Nat. Neurosci. 18, 826–835. https://doi.org/10.1038/nn.4004

Martin del Campo, H., Measor, K., Razak, K.A., 2014. Parvalbumin and calbindin expression in parallel thalamocortical pathways in a gleaning bat, Antrozous pallidus. J. Comp. Neurol. 522, 2431–2445. https://doi.org/10.1002/cne.23541

Mazzoni, E.O., Mahony, S., Closser, M., Morrison, C.A., Nedelec, S., Williams, D.J., An, D., Gifford, D.K., Wichterle, H., 2013. Synergistic binding of transcription factors to cell-specific enhancers programs motor neuron identity. Nat. Neurosci. 16, 1219–1227. https://doi.org/10.1038/nn.3467

Olsen, D., Nagayoshi, T., Fazio, M., Peltonen, J., Jaakkola, S., Sanborn, D., Sasaki, T., Kuivaniemi, H., Chu, M.L., Deutzmann, R., 1989. Human laminin: cloning and sequence analysis of cDNAs encoding A, B1 and B2 chains, and expression of the corresponding genes in human skin and cultured cells. Lab. Investig. J. Tech. Methods Pathol. 60, 772–782.

Paik, E.J., O'Neil, A.L., Ng, S.-Y., Sun, C., Rubin, L.L., 2018. Using intracellular markers to identify a novel set of surface markers for live cell purification from a heterogeneous hIPSC culture. Sci. Rep. 8, 804. https://doi.org/10.1038/s41598-018-19291-4

Pedersen, I.L., Klinck, R., Hecksher-Sorensen, J., Zahn, S., Madsen, O.D., Serup, P., Jorgensen, M.C., 2006. Generation and characterization of monoclonal antibodies

against the transcription factor Nkx6.1. J. Histochem. Cytochem. Off. J. Histochem. Soc. 54, 567–574. https://doi.org/10.1369/jhc.5A6827.2006

Previtali, S.C., Dina, G., Nodari, A., Fasolini, M., Wrabetz, L., Mayer, U., Feltri, M.L., Quattrini, A., 2003. Schwann cells synthesize alpha7beta1 integrin which is dispensable for peripheral nerve development and myelination. Mol. Cell. Neurosci. 23, 210–218.

Ryczko, D., Cone, J.J., Alpert, M.H., Goetz, L., Auclair, F., Dube, C., Parent, M., Roitman, M.F., Alford, S., Dubuc, R., 2016. A descending dopamine pathway conserved from basal vertebrates to mammals. Proc. Natl. Acad. Sci. U. S. A. 113, E2440-2449. https://doi.org/10.1073/pnas.1600684113

Sakai, A., Nakato, R., Ling, Y., Hou, X., Hara, N., Iijima, T., Yanagawa, Y., Kuwano, R., Okuda, S., Shirahige, K., Sugiyama, S., 2017. Genome-Wide Target Analyses of Otx2 Homeoprotein in Postnatal Cortex. Front. Neurosci. 11, 307. https://doi.org/10.3389/fnins.2017.00307

Sandmeier, E., Hale, T.I., Christen, P., 1994. Multiple evolutionary origin of pyridoxal-5'-phosphate-dependent amino acid decarboxylases. Eur. J. Biochem. 221, 997–1002. https://doi.org/10.1111/j.1432-1033.1994.tb18816.x

Sonnenberg, A., Janssen, H., Hogervorst, F., Calafat, J., Hilgers, J., 1987. A complex of platelet glycoproteins Ic and IIa identified by a rat monoclonal antibody. J. Biol. Chem. 262, 10376–10383.

Tan, X., Liu, W.A., Zhang, X.-J., Shi, W., Ren, S.-Q., Li, Z., Brown, K.N., Shi, S.-H., 2016. Vascular Influence on Ventral Telencephalic Progenitors and Neocortical Interneuron Production. Dev. Cell 36, 624–638. https://doi.org/10.1016/j.devcel.2016.02.023

Villaescusa, J.C., Li, B., Toledo, E.M., Rivetti di Val Cervo, P., Yang, S., Stott, S.R., Kaiser, K., Islam, S., Gyllborg, D., Laguna-Goya, R., Landreh, M., Lonnerberg, P., Falk, A., Bergman, T., Barker, R.A., Linnarsson, S., Selleri, L., Arenas, E., 2016. A PBX1 transcriptional network controls dopaminergic neuron development and is impaired in Parkinson's disease. EMBO J. 35, 1963–1978. https://doi.org/10.15252/embj.201593725

Von Ballestrem, C.G., Uniyal, S., McCormick, J.I., Chau, T., Singh, B., Chan, B.M., 1996. VLA-beta 1 integrin subunit-specific monoclonal antibodies MB1.1 and MB1.2: binding to epitopes not dependent on thymocyte development or regulated by phorbol ester and divalent cations. Hybridoma 15, 125–132. https://doi.org/10.1089/hyb.1996.15.125

Wang, Y., Gao, W., Shi, X., Ding, J., Liu, W., He, H., Wang, K., Shao, F., 2017. Chemotherapy drugs induce pyroptosis through caspase-3 cleavage of a gasdermin. Nature 547, 99–103. https://doi.org/10.1038/nature22393

Yao, Y., Chen, Z.-L., Norris, E.H., Strickland, S., 2014. Astrocytic laminin regulates pericyte differentiation and maintains blood brain barrier integrity. Nat. Commun. 5, 3413. https://doi.org/10.1038/ncomms4413

Yap, L., Wang, J.-W., Moreno-Moral, A., Chong, L.Y., Sun, Y., Harmston, N., Wang, X., Chong, S.Y., Ohman, M.K., Wei, H., Bunte, R., Gosh, S., Cook, S., Hovatta, O., de Kleijn, D.P.V., Petretto, E., Tryggvason, K., 2019. In Vivo Generation of Post-infarct Human Cardiac Muscle by Laminin-Promoted Cardiovascular Progenitors. Cell Rep. 26, 3231–3245.e9. https://doi.org/10.1016/j.celrep.2019.02.083